Multivariate ocean-climate indicators (MOCI) for the central California Current: Environmental change, 1990–2010

William J. Sydeman [a,b,c,*], Sarah Ann Thompson [a,d], Marisol García-Reyes [a], Mati Kahru [b], William T. Peterson [e], John L. Largier [c]

[a] Farallon Institute for Advanced Ecosystem Research, Petaluma, CA 94952, United States
[b] Scripps Institution of Oceanography, Integrative Oceanography Division, La Jolla, CA 95060, United States
[c] Bodega Marine Laboratory, University of California at Davis, Bodega Bay, CA 94923, United States
[d] Climate Impacts Group, College of the Environment, University of Washington, Seattle, WA 98195, United States
[e] NOAA National Marine Fisheries Service, Northwest Fisheries Science Center, Hatfield Marine Science Center, Newport, OR 97365, United States

ARTICLE INFO

ABSTRACT

Temporal environmental variability may confound interpretations of management actions, such as reduced fisheries mortality when Marine Protected Areas are implemented. To aid in the evaluation of recent ecosystem protection decisions in central-northern California, we designed and implemented multivariate ocean-climate indicators (MOCI) of environmental variability. To assess the validity of the MOCI, we evaluated interannual and longer-term variability in relation to previously recognized environmental variability in the region, and correlated MOCI to a suite of biological indicators including proxies for lower- (phytoplankton, copepods, krill), and upper-level (seabirds) taxa. To develop the MOCI, we selected, compiled, and synthesized 14 well-known atmospheric and oceanographic indicators of large-scale and regional processes (transport and upwelling), as well as local atmospheric and oceanic response variables such as wind stress, sea surface temperature, and salinity. We derived seasonally-stratified MOCI using principal component analysis. Over the 21-year study period (1990–2010), the ENSO cycle weakened while extra-tropical influences increased with a strengthening of the North Pacific Gyre Oscillation (NPGO) and cooling of the Pacific Decadal Oscillation (PDO). Correspondingly, the Northern Oscillation Index (NOI) strengthened, leading to enhanced upwelling-favorable wind stress and cooling of air and ocean surface temperatures. The seasonal MOCI related well to subarctic copepod biomass and seabird productivity, but poorly to chlorophyll-a concentration and krill abundance. Our results support a hypothesis of enhanced sub-arctic influence (transport from the north) and upwelling intensification in north-central California over the past two decades. Such environmental conditions may favor population growth for species with sub-arctic zoogeographic affinities within the central-northern California Current coastal ecosystem.

© 2013 Elsevier Ltd. All rights reserved.

1. Introduction

Ocean-climate variability has been shown to strongly affect marine life, including plankton, fish, and top predators, with clear applications in fisheries, wildlife, and ecosystem management (Hjort, 1914; Beaugrand et al., 2003; Cury et al., 2008; Carr et al., 2011). Compared to many of the world's seas, the effects of ocean-climate variability on the California Current ecosystem (CCE) have been particularly well-studied (Peña and Bograd, 2007). This marine realm, situated off the west coast of Canada, the U.S., and Baja California, Mexico, is affected by basin-scale atmospheric–oceanic coupling due to the combined effects of El

Niño Southern Oscillation events (ENSO; Lenarz et al., 1995; McPhaden et al., 2006), the decadal-scale North Pacific Gyre Oscillation (Di Lorenzo et al., 2008), and Pacific Decadal Oscillation (PDO; Mantua et al., 1997). Regional coastal and offshore upwelling also affects biotic variability of the CCE from daily to decadal time scales (Huyer, 1983; García-Reyes and Largier, 2010, 2012). Mechanistically, currents associated with tropical and extra-tropical transport bring waters of varying characteristics into the system (Chelton et al., 1982). Subsequently, regional upwelling and its vertical and offshore displacement operate on these water masses, dispersing nutrients and plankton, which in turn determines primary and secondary productivity (Checkley and Barth, 2009). Thus, to understand how climate variability relates to marine life in the CCE, consideration of the interactive effects of horizontal (currents) and vertical (upwelling) transport is required. Although a variety of indicators are available as proxies of these

processes, rarely have they been combined in a holistic manner to examine bio-physical interactions in this or other ecosystems globally (but see Hemery et al., 2008 for a multivariate approach).

Ocean-climate variability also may confound interpretations of management actions, such as reduced fisheries mortality after Marine Protected Areas are implemented. Recently, the State of California established a network of 124 Marine Protected Areas (MPAs) and 15 special closures in which fisheries and other human activities were either curtailed or eliminated entirely. This management action was taken primarily to promote the recovery of depleted groundfish (*Sebastes* spp.) and their associated ecosystem. In conjunction with implementation, an evaluation program designed to provide information on biotic responses to reductions in fisheries mortality and other factors was initiated. Though local environmental fluctuations may be important for MPAs, we focus on regional and larger scale environmental fluctuations since they have an important impact on the local ecosystem. Indeed, many of the focal *Sebastes* spp. are known to respond to variation in large-scale and local ocean climate with effects on growth (e.g., Black et al., 2011) and proxies of reproductive success (Ralston

et al., 2013). Thus, to place biological observations in an environmental context, we designed and implemented a framework for ocean-climate indicators for the central and north-central California Current by combining a suite of well-known indicators using multivariate statistical procedures (see also Mackas et al., 2007; Hemery et al., 2008). Our principal goal was to provide an assessment of environmental conditions leading up to MPA establishment in the mid-late 2000s. Because CCE biota respond to seasonal variation in environmental conditions (e.g., Hooff and Peterson, 2006; Black et al., 2010, 2011; Thompson et al., 2012), we produced indicators for variability stratified by season. The utility of complex multivariate indicators can be challenged if they are difficult to interpret or do not accurately represent known environmental variability (Rice and Rochet, 2005). Therefore, based on the literature, we developed a series of expectations to evaluate multivariate indicators. These include El Niño conditions that affected the region in 1992–1993, 1997–1998, 2003, and 2009–2010 (Bjorkstedt et al., 2010), the warm-water non-El Niño event of 2005 (GRL Special Section, 2006), and strong La Niña conditions in 1999 and 2008. These conditions have been well described in

Table 1
Data sets used. Shown for each variable is the year of the beginning of the full time series (all data sets extend through 2010) and the source for the data.

Variable type	Variable	Beginning year of time series	Data source
Sub-tropical Climate Indices	Southern Oscillation Index	1900	Climate Analysis Section, National Center for Atmospheric Research
	Multivariate El Niño-Southern Oscillation Index	1950	Earth System Research Laboratory, National Oceanic and Atmospheric Administration
	Oceanic Niño Index	1950	Center for Climate Prediction, National Weather Service, National Oceanic and Atmospheric Administration
Sub-arctic Climate Indices	North Pacific Index	1900	Climate Analysis Section, National Center for Atmospheric Research
	North Pacific Gyre Oscillation	1950	Emanuele Di Lorenzo, Georgia Institute of Technology
	Pacific Decadal Oscillation	1900	Joint Institute for the Study of the Atmosphere and Ocean, University of Washington
Upwelling	Northern Oscillation Index	1970	Pacific Fisheries Environmental Laboratory, National Oceanic and Atmospheric Administration
	Bakun Upwelling Index 36°N	1946	Environmental Research Division, National Oceanic and Atmospheric Administration
	Bakun Upwelling Index 39°N	1946	
Wind stress	Bodega Bay	1982	Marisol Garcia-Reyes, University of California Davis
	San Francisco	1982	
	Half Moon Bay	1982	
	Monterey Bay	1982	
Sea level	South Beach	1967	National Water Level Observation Network, Center for Operational Oceanographic Products and Services
	Crescent City	1933	
	San Francisco	1901	
Sea surface temperature	Point Arena	1982	National Oceanic and Atmospheric Administration
	Bodega Marine Lab	1988	Bodega Ocean Observing Node, Bodega Marine Lab, University of California Davis
	Bodega Bay	1981	National Oceanic and Atmospheric Administration
	San Francisco	1983	
	Farallon Islands	1955	Scripps Institution of Oceanography Shore Stations Program
	Half Moon Bay	1981	National Oceanic and Atmospheric Administration
	Monterey Bay	1987	
Salinity	Bodega Marine Lab	1988	Bodega Ocean Observing Node, Bodega Marine Lab, University of California Davis
	Farallon Islands	1955	Scripps Institution of Oceanography Shore Stations Program
Air temperature	Fort Ross	1950	National Climate Data Center, National Oceanic and Atmospheric Administration
	Bodega Marine Lab	1988	Bodega Ocean Observing Node, Bodega Marine Lab, University of California Davis
	San Francisco	1959	National Climate Data Center, National Oceanic and Atmospheric Administration
	Pacifica	1984	
	Half Moon Bay	1939	
Precipitation	Fort Ross	1931	National Climate Data Center, National Oceanic and Atmospheric Administration
	San Francisco	1959	
	Pacifica	1984	
	Half Moon Bay	1939	
Biological	Chlorophyll-a Concentration	1997	Mati Kahru, Scripps Photobiology Group, Scripps Institution of Oceanography
	Northern Copepod Index	1996	William Peterson, Northwest Fisheries Science Center, National Oceanic and Atmospheric Administration
	Krill Abundance	1990	John Field, Southwest Fisheries Science Center, National Oceanic and Atmospheric Administration
	Seabird Reproductive Success	1971, 1972	Point Blue Conservation Science

previous publications, but to date there have been no attempts to create multivariate ocean-climate indicators or evaluate how well these indicators represent such variability. If indicators match known variability, arguably they would be interpretable and representative, key attributes for useful and valid ecological indicators (Levin et al., 2009). To test the utility of our multivariate ocean-climate indicators (hereafter MOCI, see Hemery et al., 2008), we related them to four biological indicators from multiple trophic levels.

2. Methods

We focused data synthesis on 1990 through 2010 as this period followed the putative regime shifts of 1989–1990 (Hare and Mantua, 2000) and 1976–1977 (McGowan et al., 2003). Others have suggested another regime shift in 1998–1999 (Bond et al., 2003; Peterson and Schwing, 2003; Chavez et al., 2011), but the persistence of this shift remains equivocal. We selected a total of 14 basin- (SOI, MEI, ONI, NPI, PDO, NPGO, and NOI) and regional-scale (Upwelling Index, wind stress, sea level, SST, salinity, surface air temperature, and precipitation) atmospheric and oceanographic indicators for synthesis (Table 1, see below for descriptions). We evaluated environmental conditions by exploring variability on seasonal and interannual time scales. We focused on understanding the status of the environment in considering the potential for rapid biological responses to immediate reduced fisheries mortality associated with the establishment of MPAs. However, while some rapid responses are possible, long-lived species may not show many short-term changes. This is certainly true for the *Sebastes* spp. of interest in this ecosystem – changes in the popula-

tions of these species are likely on decadal scales. Therefore, in this context, we focused on understanding trends in the environment on the interannual to decadal scale. Last, we examine the potential for the multivariate ocean climate indicators to predict biological responses by investigating relationships with four well-known biological indicators: chlorophyll-a concentrations (Kahru et al., 2012), copepod biomass (Hooff and Peterson, 2006), krill abundance (Santora et al., 2012), and seabird reproductive success (Sydeman et al., 2001).

2.1. Data

2.1.1. Indicators of transport from the tropics

Indicators of the warm El Niño phase of the ENSO cycle are associated with strong advection from the tropics, whereas indicators of the cold La Niña phase reflect weak northward transport. We used three indicators for El Niño: one atmospheric, one oceanographic, and one multivariate indicator that includes both oceanographic and atmospheric variables. The Southern Oscillation Index (SOI), calculated as monthly fluctuations in sea level pressure between the Tahiti Low and Darwin, Australia High, was used as an indicator of the atmospheric drivers of ENSO. Prolonged negative values signify El Niño episodes while sustained positive values are associated with La Niña episodes. To present the SOI in phase with other variables, we reversed the sign of this indicator, such that positive values reflect El Niño and negative values reflect La Niña. Data were calculated by the Climate Analysis Section, National Center for Atmospheric Research, and were obtained from http://www.cgd.ucar.edu/cas/catalog/climind/SOI.signal.ascii. The Oceanic Nino Index (ONI), a 3-month running mean of SST anomalies in the region 5°N–5°S, 120–170°W (Nino3.4), was used as an
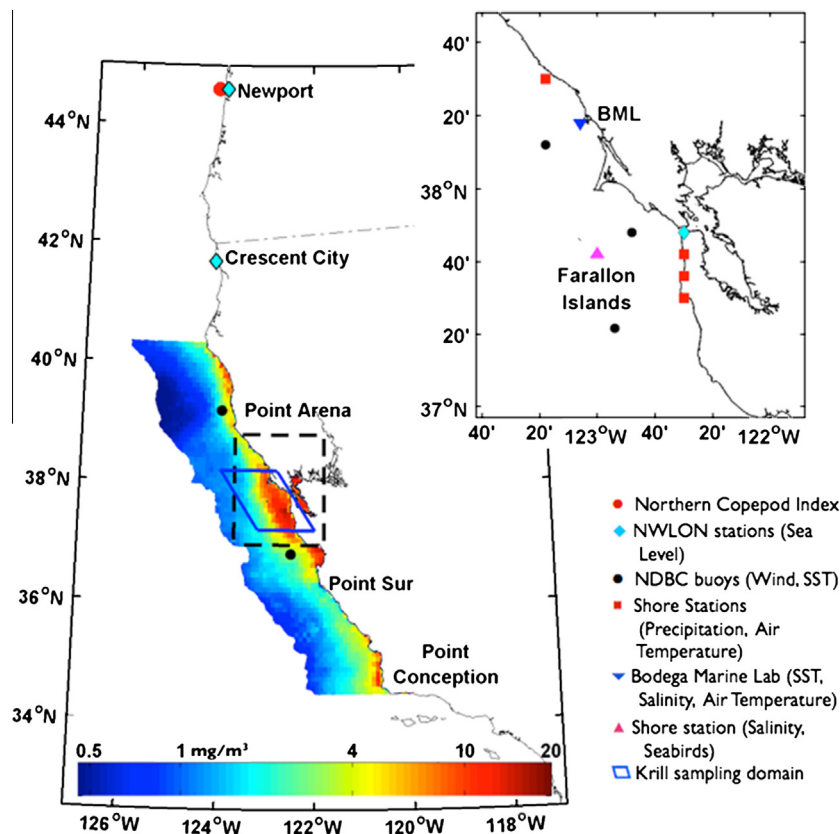
Fig. 1. Map of the study area showing data locations and domains for physical and biological variables used in the development of seasonal MOCI. The color bar indicates average May–July chl-a concentration for 1998–2010. Inset is the greater Gulf of the Farallones region. (For interpretation of the references to color in this figure legend, the reader is referred to the web version of this article.)

oceanographic manifestation of the ENSO cycle. The ONI is computed by the NOAA National Weather Service, Center for Climate Prediction. Data were obtained from http://www.cpc.ncep.noaa.-gov/products/analysis_monitoring/ensostuff/ensoyears.shtml. The Multivariate ENSO Index (MEI), based on six observed variables over the tropical Pacific, was used as an indicator of the tropical oceanographic manifestation of the ENSO cycle (Wolter and Timlin, 1993). Negative values of the MEI represent the cold ENSO phase (La Niña) while positive MEI values represent the warm ENSO phase (El Niño). Data were obtained from NOAA's Earth System Research Laboratory at http://www.esrl.noaa.gov/psd/enso/mei/table.html.

2.1.2. Indicators of transport from the extra-tropics

We selected the North Pacific Index (NPI), the area-weighted sea level pressure over the region 30°N–65°N, 160°E–140°W, as our atmospheric driver of transport from the North Pacific to the California Current. Data were calculated by the Climate Analysis Section, National Center for Atmospheric Research and were downloaded from http://www.cgd.ucar.edu/cas/jhurrell/indices.data.html#npmon. This variable provides an index of the strength and positioning of the Aleutian Low Pressure system, which in turn is expressed in large-scale ocean conditions in the North Pacific reflected in the Pacific Decadal Oscillation (PDO) and North Pacific Gyre Oscillation Index (NPGO). The NPGO index was downloaded from http://eros.eas.gatech.edu/npgo/data/NPGO.txt and emerges as the second EOF of Northeast Pacific sea-surface height anomalies (Di Lorenzo et al., 2008). Positive values also indicate a strong North Pacific gyre and advective transport from the north (Hooff and Peterson, 2006; Keister et al., 2011). We also used the PDO index, developed by Zhang et al. (1997), as an oceanographic index of sub-arctic influences on the CCE. Data were downloaded from the Joint Institute for the Study of the Atmosphere and Ocean at the University of Washington. Methods and details of computation are available at http://jisao.washington.edu/pdo/PDO.latest. The PDO reflects SST for the entire North Pacific, including the CCE, at locations >20°N. Positive values of the PDO indicate warm SST along the eastern north Pacific and cool SST over the central and western north Pacific.

2.1.3. Indicators of regional upwelling

The Northern Oscillation Index (NOI) provides an index of the strength and positioning of the North Pacific High pressure system (Schwing et al., 2002; Schroeder et al., 2013) which, with the Continental Thermal Low, drives the winds that cause upwelling in north-central California. The NOI is also an indicator to tropical climate variability, ENSO, and equatorial trade winds (Schwing et al., 2002). The index is calculated by the Pacific Fisheries Environmental Laboratory, NOAA, based on monthly fluctuations in the sea level pressure difference between the North Pacific High and Darwin (Australia) Low thus also including variability from the tropics. NOI data were downloaded from http://www.pfeg.noaa.gov/products/PFEL/modeled/indices/NOIx/noix_download.html. The amplitude of upwelling is proxied by the Upwelling Index (UI), calculated by NOAA's Environmental Research Division, from estimates of the magnitude of wind stress derived from pressure gradients (Schwing et al., 1996, 2006; Bograd et al., 2009). Positive values indicate upwelling while negative values indicate downwelling. We downloaded UI data for 36°N 122°W and 39°N 125°W from ftp://orpheus.pfeg.noaa.gov/outgoing/upwell/monthly/upindex.mon.

We used monthly alongshore wind stress as an index of upwelling-favorable winds in the region. García-Reyes and Largier (2010, 2012) calculated this variable based on wind speed and direction measured at NOAA buoys at Point Arena (Fig. 1; 39.2°N 124.0°W), Bodega Bay (38.2°N 123.3°W), San Francisco (37.8°N

122.8°W), and Half Moon Bay (37.4°N 122.9°W). Negative values indicate wind stress in an upwelling-favorable equatorial direction, but for better interpretation of this variable we reversed the sign to make it in phase with other indicators. Details of the methodology can be found in García-Reyes and Largier (2010, 2012).

2.1.4. Indicators of local hydrographic conditions

Sea level measurements (mm), compiled by the National Water Level Observation Network (NWLON), were obtained from the Center for Operational Oceanographic Products and Services (CO-OPS; NOS, 2008). We used monthly data, which represent an average of daily values, from the San Francisco (Fig. 1; 37.8°N 122.5°W), Crescent City (41.4°N 124.1°W), and South Beach (44.4°N 124.0°W) sea level gauges. Methods and data were downloaded from the University of Hawaii Sea Level Center (http://www.uhslc.soest.hawaii.edu/). Local sea level also indexes upwelling and transport.

Sea surface temperature data (SST; °C) were collected from the Farallon Islands shore station (Fig. 1; 37.7°N 123°W), NOAA buoys (Point Arena (39.2°N 124.0°W), Bodega Bay (38.2°N 123.3°W), San

Table 2
Trends for physical variables based on Spearman rank correlation, 1990 to 2010 ($n = 252$ months). p-values were calculated with Monte Carlo randomization simulations; shading indicates significance ($p < 0.05$). Climate indices and the Northern Oscillation Index were subjected to quadratic regression to test for non-linearity in patterns of change (* denotes variables with significant quadratic terms).

	Spearman rho	p-value
Sub-tropical Climate Indices		
Southern Oscillation Index*	−0.31	<0.01
Multivariate ENSO Index*	−0.31	<0.01
Oceanic Nino Index*	−0.20	<0.01
Sub-arctic Climate Indices		
North Pacific Index	0.08	0.22
North Pacific Gyre Oscillation*	0.52	<0.01
Pacific Decadal Oscillation*	−0.25	<0.01
Upwelling		
Northern Oscillation Index*	0.28	<0.01
Bakun Upwelling Index 36°N	0.11	0.07
Bakun Upwelling Index 39°N	0.17	0.01
Wind stress		
Bodega Bay	0.13	0.03
San Francisco	0.20	<0.01
Half Moon Bay	0.18	<0.01
Monterey Bay	0.15	0.02
Sea level		
South Beach	0.03	0.62
Crescent City	−0.27	<0.01
San Francisco	0.00	0.99
Sea surface temperature		
Point Arena	−0.24	<0.01
Bodega Marine Lab	−0.08	0.19
Bodega Bay	−0.17	<0.01
San Francisco	−0.09	0.15
Farallon Islands	−0.20	<0.01
Half Moon Bay	−0.17	<0.01
Monterey Bay	0.02	0.75
Salinity		
Bodega Marine Lab	0.08	0.16
Farallon Islands	0.01	0.87
Air temperature		
Fort Ross	−0.03	0.68
Bodega Marine Lab	−0.35	<0.01
San Francisco	−0.20	<0.01
Pacifica	0.17	<0.01
Half Moon Bay	−0.07	0.30
Precipitation		
Fort Ross	0.06	0.36
San Francisco	0.04	0.49
Pacifica	0.01	0.91
Half Moon Bay	0.00	1.00

Francisco (37.8°N 122.8°W), Half Moon Bay (37.4°N 122.9°W), and Monterey Bay (36.8°N 122.4°W)), and the Bodega Ocean Observing Node (BOON) program at the UC Davis Bodega Marine Lab (38.3°N 123.1°W). Methods and data for the Farallon Islands shore station are available from http://shorestation.ucsd.edu/methods/index_methods.html. Buoy data were downloaded from the National Data Buoy Center (http://www.ndbc.noaa.gov/) and Bodega Marine Lab SST data were downloaded from http://bml.ucdavis.edu/boon/data_seatemp.html. Salinity data (psu) from the Farallon Islands (Fig. 1; 37.7°N 123°W) and the Bodega Marine Lab (BML; 38.3°N 123.1°W) were also compiled. Data were downloaded from ftp://ftp.iod.ucsd.edu/shore/active_data/farallon/salinity/ and http://bml.ucdavis.edu/boon/data_salinity.html, respectively. Air temperature (°C) was measured at the Bodega Marine Lab (38.3°N 123.1°W) in a weather box 40 m from the coastal bluff. Data were obtained from http://bml.ucdavis.edu/boon/data_airtemp.html. Daily temperatures were averaged to monthly values for analysis. Lastly, precipitation (cm) and air temperature (°C) data were downloaded from the National Climate Data Center, NOAA (http://cdo.ncdc.noaa.gov/pls/plclimprod/somdmain.somdwrapper?datasetabbv=DS3220&countryabbv=&georegionabbv=&forceoutside) for sites at Fort Ross (Fig. 1; 38.5°N 123.3°W), San Francisco (37.7°N 122.5°W), Pacifica (37.6°N 122.5°W), and Half Moon Bay (37.5°N 122.5°W).

2.1.5. Lower trophic level indicators

We used a data set of regional satellite-derived chlorophyll-a (chl-a) combined from multiple sources to proxy phytoplankton biomass; methods for the compilation of chl-a data are described by Kahru et al. (2012). The compilation domain was coastal from 34° to 40°N, to 100 km offshore (Fig. 1). Briefly, long term measure-

ments of chl-a were obtained in situ and via satellite-borne sensors of ocean color. Outputs from OCTS, SeaWiFS, MODIS-Aqua, and MERIS were obtained and algorithms created to facilitate sensor compatibility. Further, 10,050 near-surface in situ chl-a measurements taken from ships from 1996 through 2010 were used to calibrate the satellite-derived values. All satellite sensors showed strong positive correlations with in situ data. Merged daily data were composited into monthly data sets. We log_{10} transformed monthly chl-a concentration data to account for the log-normal distribution and calculated seasonal averages from monthly data: spring (February–April), summer (May–July), fall (August–October) and winter (November–January). These "seasons" differ slightly from those developed for environmental indicators (see below). We did this to provide a 1-month lag between our chl-a concentration and environmental conditions.

Copepods were sampled bi-weekly at a hydrographic station five miles off Newport, Oregon, from 1996 through 2010 (Fig. 1). Calculation of the Northern Copepod Index (NCI) is the monthly mean log biomass anomaly of three species of lipid-rich, boreal, cold-water copepods: *Calanus marshallae*, *Pseudocalanus mimus*, and *Acartia longiremis* (Hooff and Peterson, 2006). For our analyses, we averaged monthly NCI data into the same seasons as those for phytoplankton.

Data on the relative abundance of krill were obtained from the National Marine Fisheries Service Juvenile Rockfish – Ecosystem survey conducted annually in the region of Point Sur to Point Arena, CA from 1983 – present (see maps in Sakuma et al., 2006; Field et al., 2010; Ralston et al., 2013). Estimates of krill abundance were derived from mid-water (~30 m) trawls at 14 stations regularly occupied in the area (Fig. 1; Santora et al., 2012). From these
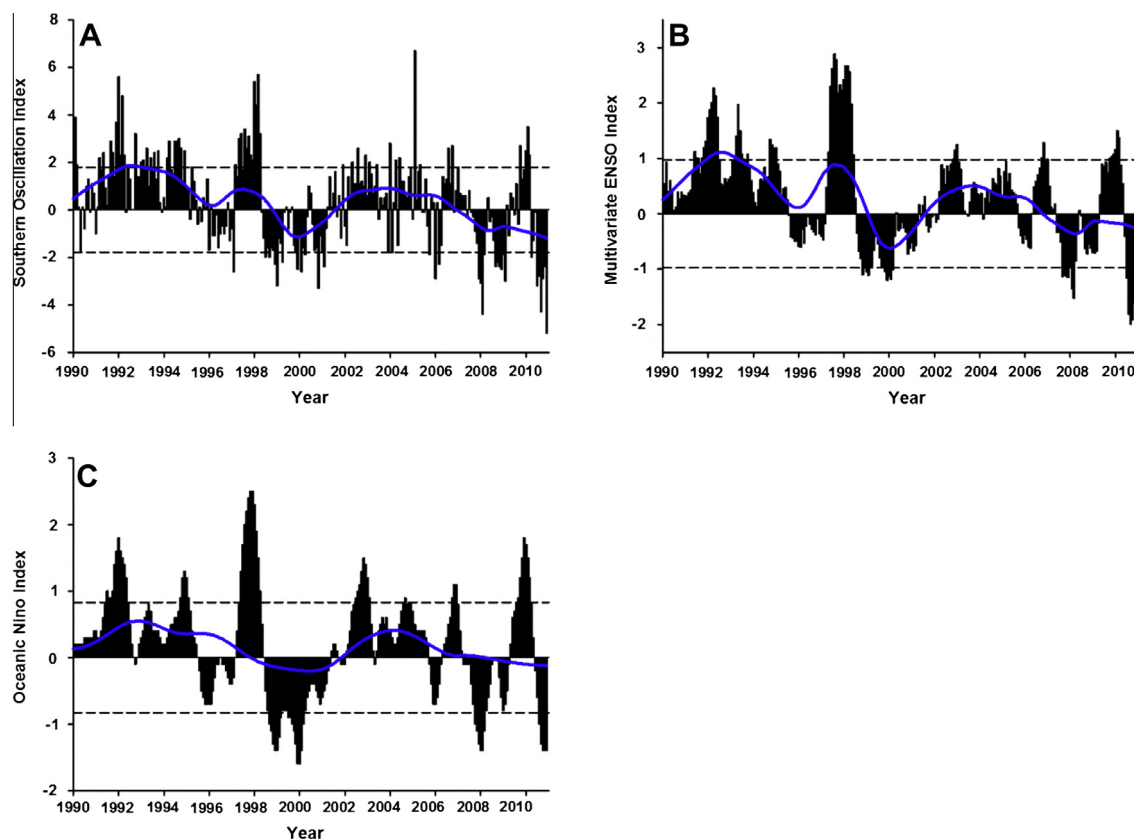
Fig. 2. Indicators of El Niño/La Niña, transport from the tropics. (A) Southern Oscillation Index (SOI, sign reversed), (B) multivariate ENSO Index (MEI), and (C) Oceanic Niño Index (ONI), 1990–2010. Blue line indicates LOESS smoothing function with sampling proportion of 0.2. Dashed lines show ±1 long-term standard deviation based on time series of varying lengths: (SOI: 1900–2010, MEI and ONI: 1950–2010). (For interpretation of the references to color in this figure legend, the reader is referred to the web version of this article.)

stations, data from a total of 912 trawls from 1990 to 2008 were summarized (García-Reyes et al., in press). For each tow, krill were separated from the catch of fish, volumetrically sub-sampled, and enumerated. We calculated the annual geometric mean as the average of ln(number individuals haul^{-1}) from 1990 to 2008. This krill index reflects the abundance of three species: *Euphausia pacifica*, *Thysanoessa spinifera*, and *Nyctiphanes simplex*; species data are not available for the time series used in this analysis.

2.1.6. Upper trophic level indicators

Breeding success data for seabirds including common murre (*Uria aalge*), pigeon guillemot (*Cepphus columba*), Cassin's auklet (*Ptychoramphus aleuticus*), and Brandt's cormorant (*Phalacrocorax penicillatus*) were obtained from studies at Southeast Farallon Island, CA (37.7°N 123°W) (Fig. 1; Sydeman et al., 2001; Bjorkstedt et al., 2012). Reproductive success is defined as the number of offspring departing the colony per breeding pair per year. Data were available for 1971–2007 for all species except common murre, which were available for 1972–2007.
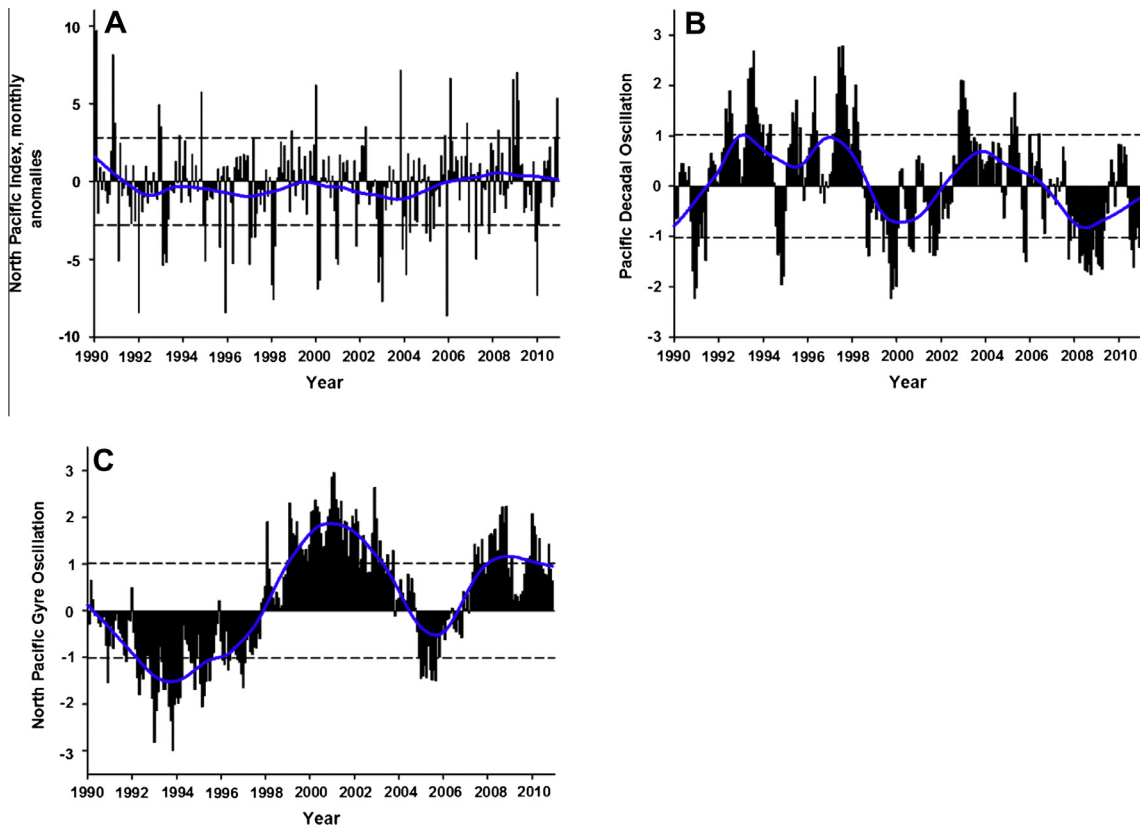
Fig. 3. Indicators of transport from the sub-arctic North Pacific. (A) North Pacific Index (NPI) monthly anomalies, (B) Pacific Decadal Oscillation (PDO), and (C) North Pacific Gyre Oscillation Index (NPGO), 1990–2010. Blue line indicates LOESS smoothing function with sampling proportion of 0.2. Dashed lines show ±1 long-term standard deviation based on varying time series (NPI and PDO: 1900–2010 and NPGO: 1950–2010). (For interpretation of the references to color in this figure legend, the reader is referred to the web version of this article.)
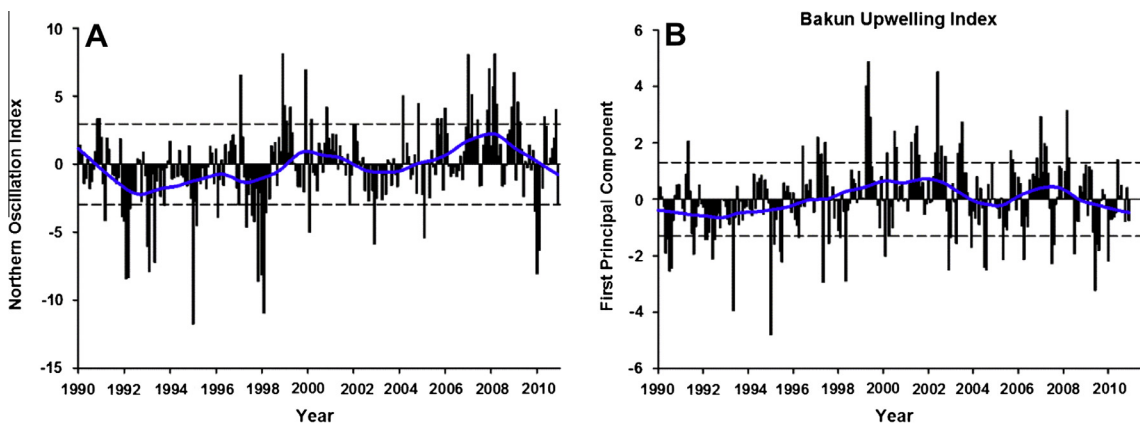
Fig. 4. (A) Indicators of regional upwelling. Northern Oscillation Index (NOI) and (B) the first principal component of Bakun Upwelling Index at 36°N and 39°N, 1990–2010. Blue line indicates LOESS smoothing function with sampling proportion of 0.2. Dashed lines show ±1 long-term standard deviation for NOI (1970–2010) and 1990–2010 standard deviation for Upwelling PC1. (For interpretation of the references to color in this figure legend, the reader is referred to the web version of this article.)
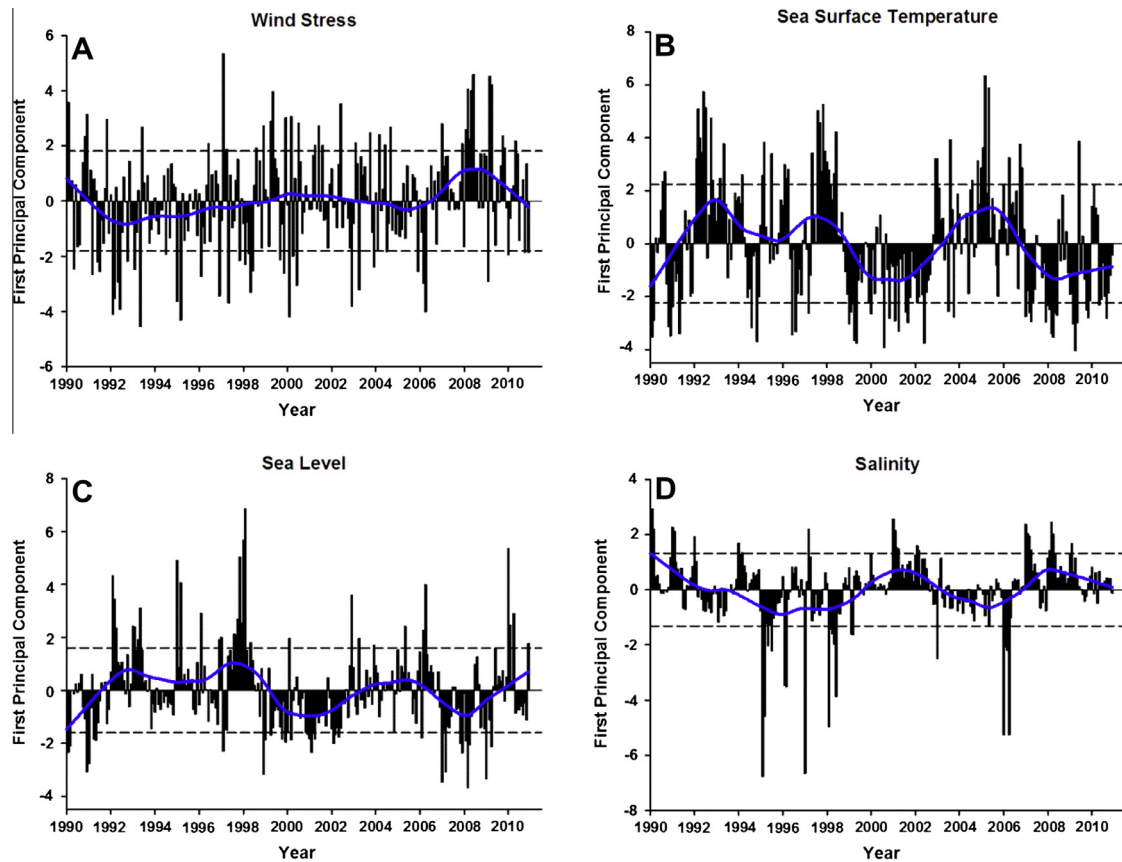
Fig. 5. Indicators of regional coupled wind and hydrography (1990–2010). First principal components were generated from principal component analysis on multiple sites for (A) wind stress, (B) sea surface temperature, (C) sea level, and (D) salinity. Blue line indicates LOESS smoothing function with sampling proportion of 0.2. Dashed lines show ±1 standard deviation. (For interpretation of the references to color in this figure legend, the reader is referred to the web version of this article.)
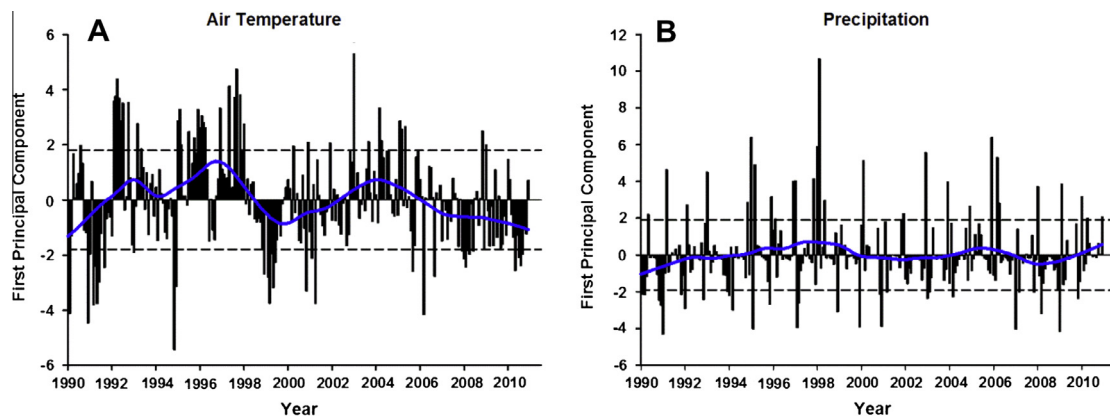
Fig. 6. Indicators of regional atmospheric conditions. First principal components were generated from principal component analysis on multiple sites for (A) air temperature and (B) precipitation, 1990–2010. Blue line indicates LOESS smoothing function with sampling proportion of 0.2. Dashed lines show ±1 standard deviation. (For interpretation of the references to color in this figure legend, the reader is referred to the web version of this article.)

2.2. Data processing and statistical analyses

2.2.1. Multivariate ocean-climate indicators (MOCI)

Monthly measurements of environmental conditions were expressed as anomalies (monthly value – long-term monthly average; based on full length of time series, see Table 1). To create the seasonal MOCI, we averaged across months for the following seasons: winter (January–March), spring (April–June), summer (July–September), and fall (October–December). Residuals of seasonal averages were calculated and used in a principal component analysis (PCA) conducted on all oceanic and atmospheric variables, by season, for the years 1990–2010. The unrotated first and second principal components (MOCI1 and MOCI2) for each season were extracted and retained. The seasonal MOCI described above used the full suite of climate variables, from large-scale indices to local-scale measurements. We also generated two additional sub-groups of seasonal MOCI using PCA from (1) only the large-scale climate indices and (2) only the regional-local measurements. Subsequently, we cross-correlated these sub-groups with the original MOCI of the full suite of large-scale as well as local climate

variables to investigate similarities and differences between these approaches. As we were primarily interested in environmental conditions leading up to the growing season each year (∼March–August), we examined cross-correlations of the MOCI with the sub-groups for fall of $year_{x-1}$ and winter, spring, and summer of $year_x$.

2.2.2. Biological variables

We tested for trends in biological data sets using Spearman rank correlation. For any data set with significant time trends, we detrended and saved the residuals for further analysis. Seasonal chl-a data were detrended using quadratic regression. Linear trends were found in spring and summer NCI, so all seasons were detrended with linear regression. Krill abundance was tested for linear and quadratic trends, but none were found. To prevent possible biased results, seabird data were also de-trended using quadratic regression. The seabird residual data were further synthesized using PCA; the first principal component ($PC1_{seabirds}$), an indicator of community breeding performance (Sydeman et al., 2001), was used for analyses.

Table 3

Seasonal multivariate ocean-climate indicators (MOCI) derived by principal component analysis (PCA) of de-trended physical variables, 1990–2010. (A) Eigenvalues and proportion explained for the first and second principal components. (B) Eigenvector loadings for first and second principal components by season. Shading indicates values > |0.2|.

Season	Component	Eigenvalue	Proportion	Cumulative
(A)				
Winter	1	18.943	0.557	0.557
	2	5.000	0.147	0.704
Spring	1	18.163	0.534	0.534
	2	4.628	0.136	0.670
Summer	1	13.025	0.383	0.383
	2	4.673	0.138	0.521
Fall	1	13.729	0.404	0.404
	2	4.084	0.120	0.524

	Winter		Spring		Summer		Fall	
	1	2	1	2	1	2	1	2
(B)								
Sub-tropical Climate Indices								
Southern Oscillation Index	0.149	0.113	0.063	0.248	0.111	−0.200	0.148	0.305
Multivariate ENSO Index	0.164	0.087	0.151	0.151	0.193	−0.132	0.147	0.330
Oceanic Nino Index	0.161	0.120	0.125	0.191	0.176	−0.195	0.135	0.364
Sub-arctic Climate Indices								
North Pacific Index	−0.145	0.014	−0.078	−0.206	−0.182	0.199	−0.090	−0.091
North Pacific Gyre Oscillation	−0.073	−0.162	−0.147	−0.097	−0.071	−0.129	−0.102	0.036
Pacific Decadal Oscillation	0.157	0.206	0.182	0.028	0.196	0.031	0.219	0.012
Upwelling								
Northern Oscillation Index	−0.218	0.046	−0.191	−0.122	−0.164	0.185	−0.207	−0.262
Bakun Upwelling Index 36°N	−0.174	0.017	−0.192	−0.002	−0.136	−0.057	−0.122	−0.068
Bakun Upwelling Index 39°N	−0.193	0.111	−0.211	−0.008	−0.189	0.081	−0.110	0.074
Wind stress								
Bodega Bay	−0.193	0.119	−0.180	0.083	−0.076	0.265	−0.196	0.195
San Francisco	−0.193	0.147	−0.191	0.106	−0.027	0.152	−0.199	0.181
Half Moon Bay	−0.190	0.139	−0.141	0.011	0.052	0.218	−0.187	0.151
Monterey Bay	−0.177	0.137	−0.191	0.071	0.007	0.225	−0.204	0.081
Sea level								
South Beach	0.200	−0.142	0.199	0.001	0.251	−0.008	0.169	0.224
Crescent City	0.219	−0.086	0.222	0.017	0.235	0.039	0.212	0.172
San Francisco	0.213	−0.089	0.202	−0.102	0.179	0.203	0.225	0.224
Sea surface temperature								
Point Arena	0.192	0.057	0.184	0.048	0.236	−0.070	0.198	−0.042
Bodega Marine Lab	0.204	0.129	0.209	0.037	0.210	0.070	0.220	−0.034
Bodega Bay	0.196	0.165	0.222	−0.034	0.173	0.213	0.194	−0.159
San Francisco	0.188	0.157	0.211	0.087	0.242	0.141	0.219	−0.106
Farallon Islands	0.215	0.092	0.204	0.024	0.240	0.092	0.218	−0.019
Half Moon Bay	0.148	0.166	0.168	0.065	0.184	0.233	0.171	−0.211
Monterey Bay	0.171	0.187	0.184	−0.055	0.205	0.098	0.144	0.004
Salinity								
Bodega Marine Lab	−0.170	0.125	−0.169	0.138	−0.158	−0.038	−0.129	0.164
Farallon Islands	−0.138	0.059	−0.183	0.179	−0.124	−0.261	−0.103	0.200
Air temperature								
Fort Ross	0.169	0.169	0.162	0.191	0.199	0.059	0.157	−0.121
Bodega Marine Lab	0.151	0.178	0.172	0.151	0.094	0.115	0.197	−0.180
San Francisco	0.150	0.169	0.184	0.169	0.226	0.057	0.167	−0.205
Pacifica	0.086	0.316	0.024	0.371	0.213	−0.006	0.099	−0.209
Half Moon Bay	0.179	0.149	0.189	0.138	0.224	−0.029	0.190	−0.076
Precipitation								
Fort Ross	0.138	−0.287	0.166	−0.244	0.131	−0.207	0.118	0.144
San Francisco	0.144	−0.315	0.087	−0.359	0.133	−0.271	0.130	0.138
Pacifica	0.129	−0.338	0.122	−0.358	0.092	−0.330	0.155	0.115
Half Moon Bay	0.129	−0.323	0.108	−0.381	0.055	−0.327	0.180	0.066

2.2.3. MOCI compared to biological variables

We correlated the seasonal MOCI with the biological indicators using Spearman rank correlations. Seasonal chl-a and NCI residuals were compared to the seasonal MOCI with a 1-season lag. Krill abundance, seabird species residual data, and PC1$_{seabirds}$ were tested against the seasonal MOCI of the same year. To adjust for potential autocorrelation, all p-values were confirmed using Monte Carlo randomization procedures (Manly, 2007).

3. Results

3.1. Status and trends in basin-scale indicators

The SOI, MEI, and ONI showed negative trends (Table 2, Fig. 2), indicating a decrease in the frequency and amplitude of El Niño events. The 2010 values for the SOI and MEI were particularly anomalous (almost 2× standard deviation), indicating a strong La Niña event in that year. However, this followed a moderate El Niño from mid-2009 through early 2010. For extra-tropical indices, the NPI showed no trend (Table 2, Fig. 3a) while the PDO decreased (indicating cooling of the eastern Pacific, Fig. 3b). The NPGO increased (indicating greater gyre transport) with a distinct step from negative to mostly positive values in early 1998 (Table 2, Fig. 3c) and showed a strong period of transport from early 1999 to early 2003, which corresponds to negative PDO values during the same time period. The NPGO has been largely positive since

early 2010, in concert with a negative PDO. Changes in the NPGO and PDO during the El Niño of 2009 were not particularly noteworthy (i.e., well within 1 s.d. of the mean), though the PDO turned positive during this event.

3.2. Status and trends in regional upwelling indicators

The NOI increased in the study period though the overall rate of change was small (Table 2, Fig. 4a). The NOI was strongly negative (indicating a weak North Pacific High) in early 2010, corresponding to the 2009–2010 El Niño, but rebounded to normal levels later in the year. The NOI was particularly high from mid-2007 to early 2009, and was low but not outside 1 s.d. of the mean from late 2002 through 2006. Similar to the NOI, the UI at 36°N and 39°N had slight positive trends, and the trend for 39°N was significant (Table 2, Fig. 4b). Strong negative values in late 2009 indicate downwelling during the 2009–2010 El Niño, and the highest values were observed from 1999 through 2002.

3.3. Status and trends in regional wind and hydrographic indicators

Clear trends were observed for wind stress and SST (Table 2, Fig. 5a and b). Wind stress increased significantly at all sites and was particularly strong in 2008 but decreased in 2009. SST decreased significantly at four of seven locations over the 21-year period and was particularly low for the period 2007–2010. The
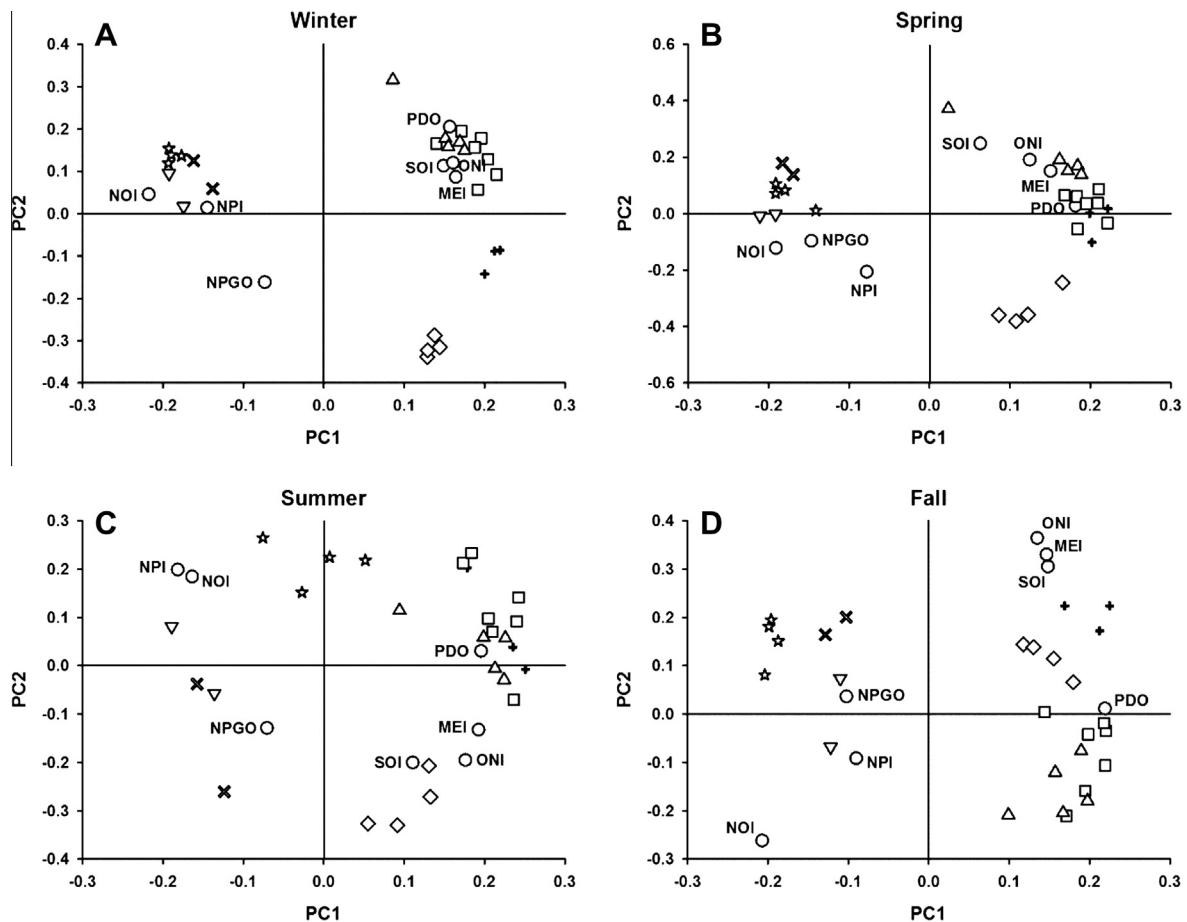
Fig. 7. The first principal component variable loadings plotted against the second principal component variable loadings (PC space) for the seasonal MOCI, 1990–2010. The MOCI were calculated from residuals of seasonal averages. (A) Winter, (B) spring, (C) summer, and (D) fall. Labels for circular symbols indicate climate variables. SOI: Southern Oscillation Index; MEI: Multivariate ENSO Index; NOI: Northern Oscillation Index; NPGO: North Pacific Gyre Oscillation; NPI: North Pacific Index; ONI: Oceanic Nino Index; PDO: Pacific Decadal Oscillation. +: sea level; squares: sea surface temperature (SST); x: salinity; triangles pointing down: Bakun Upwelling Index; stars: wind stress; triangles pointing up: air temperature; diamonds: precipitation.

only significant change in sea level, however, was decreasing sea level at Crescent City (Table 2, Fig. 5c). Sea level was elevated in late 2009, corresponding to the El Niño event at that time, but has since decreased. There were no significant trends for salinity (Fig. 5d). Corresponding to the cold SST, salinity in recent years has also been elevated but decreased from 2007 to 2010 and was not outside average values in most of 2009 and 2010.

3.4. Status and trends in regional air temperature and precipitation indicators

Air temperature at four sites decreased (Table 2, Fig. 6a), while Pacifica had increasing air temperature. Air temperature was generally low from 2008 to 2010. There were no trends in precipitation (Fig. 6b).

3.5. Development of seasonal multivariate ocean-climate indicators (MOCI)

Due to seasonal variation, we used PCA to create linear combinations of all physical variables within seasons (Table 3). There were distinct differences in the MOCI created for winter (January–March) and spring (April–June) versus summer (July–September) and fall (October–December). The eigenvalues for winter and spring were >18 whereas summer and fall were <14; this related to greater variance explained in the first two seasons (56% and 53%, respectively) compared to the latter seasons (38% and 40%, respectively; Table 3a). The second principle component for each seasonal MOCI were balanced with eigenvalues >4, and the

variance explained by each was ~13.5%. MOCI1-winter appeared to be explained primarily by a weak NOI (weak North Pacific High) and positive sea level and SST (Table 3b, Fig. 7a). We interpret MOCI1-winter as an index of wintertime atmospheric pressure and upwelling. MOCI2-winter was explained primarily by variation in precipitation (Table 3b); we therefore interpret MOCI2-winter as an indicator of local winter atmospheric conditions, including the PDO. MOCI1-spring appeared to be explained primarily by negative upwelling at 39°N and positive sea level and SST (Table 3b, Fig. 7b). Thus, we interpret MOCI1-spring also as an index of upwelling and its oceanic signatures, variation in sea level and SST (high and warm). MOCI2-spring was explained primarily by variation in SOI (positive) and NPI (negative; Table 3b), as well as precipitation. MOCI1-summer appeared to be explained primarily by positive sea level, SST, and air temperature (Table 3b, Fig. 7c). We interpret MOCI1-summer as an index of temperature. MOCI2-summer was explained primarily by weak (positive) wind stress coupled with temperature and precipitation (Table 3b). Last, MOCI1-fall appeared to be related to the PDO (positive), NOI (negative), weak wind stress, and positive sea level and SST (Table 3b, Fig. 7d), reflecting weak upwelling conditions. MOCI2-fall was explained primarily by variation in SOI, MEI, and ONI (Table 3b); therefore, we interpret MOCI2-fall as an indicator of ENSO conditions.

3.6. Trends in the MOCI

Variability in the seasonal MOCI is depicted in Fig. 8. MOCI1-winter showed strong upwelling in 1990 and 2007–2008, and
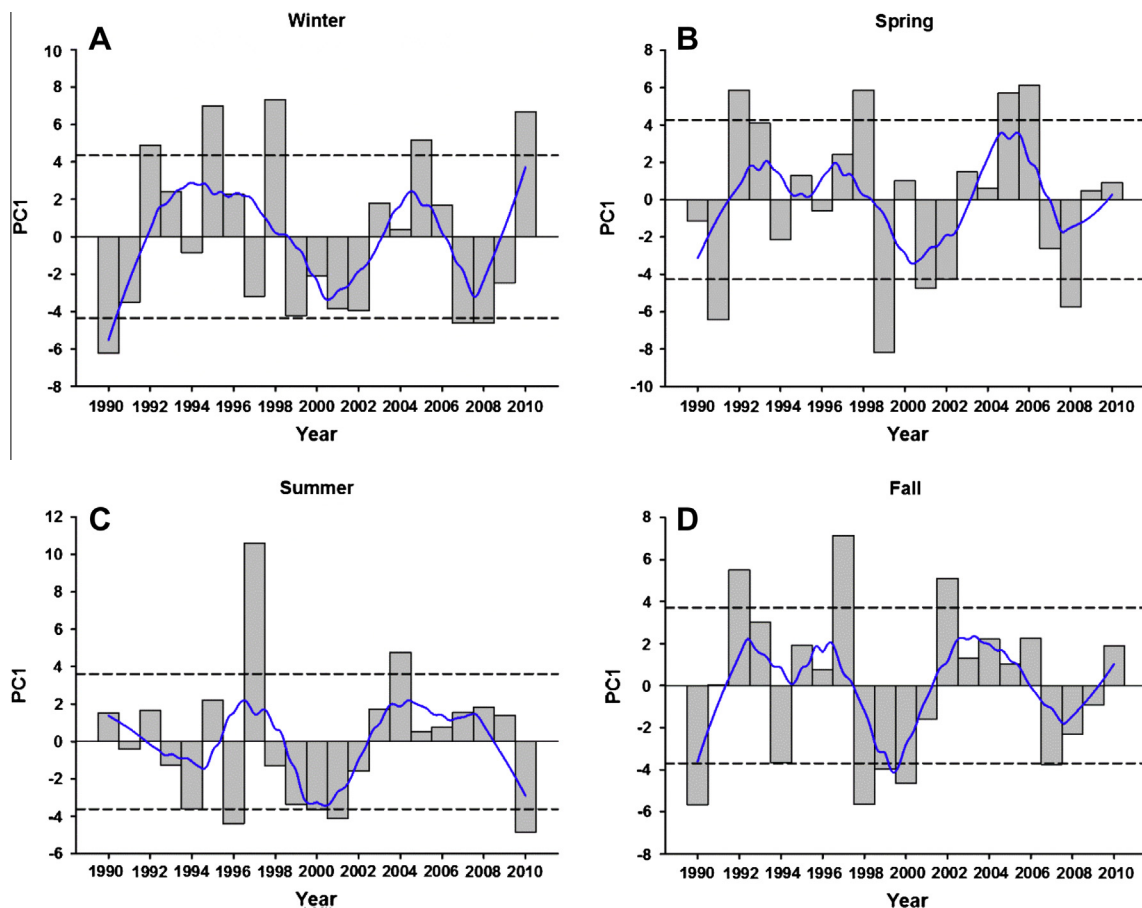
Fig. 8. The seasonal MOCI against time for (A) winter, (B) spring, (C) summer and (D) fall, 1990–2010. The MOCI were calculated from residuals of seasonal averages. Blue line shows LOESS smoothing function with sampling proportion of 0.3. Dashed lines show ±1 standard deviation. (For interpretation of the references to color in this figure legend, the reader is referred to the web version of this article.)
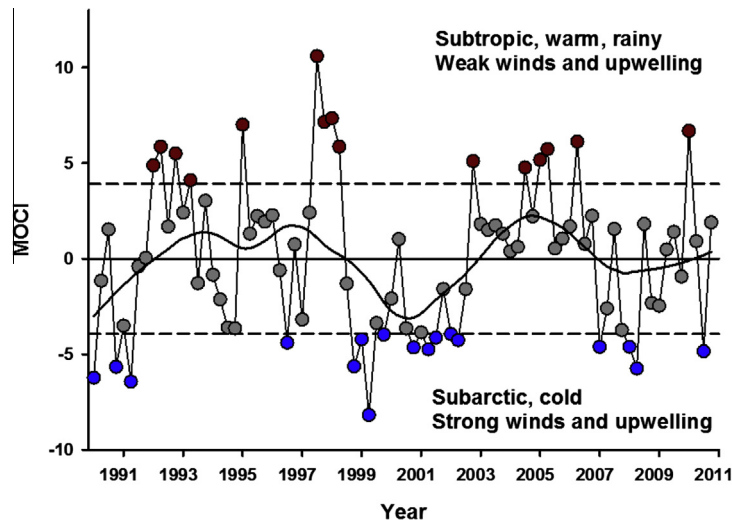
Fig. 9. The seasonal MOCI time series, 1990–2010. Smoothed line is based on LOESS with sampling proportion of 0.3. Dashed lines are 1 s.d. for the time series. 1 standard deviation was also calculated for each season. Red points indicate values greater than 1 seasonal s.d. and blue points indicate values less than 1 seasonal s.d.

Table 4
Cross-correlations of seasonal MOCI, local variables only (combined with PCA), and climate indices only (combined with PCA). In each cell, Spearman rho is the top value and the p-value is below. Shading indicates significance ($p < 0.05$). Winter, spring, and summer $n = 21$; fall $n = 20$.

	Fall$_{x-1}$		Winter		Spring		Summer	
	MOCI	Local variables	MOCI	Local variables	MOCI	Local variables	MOCI	Local variables
Local variables	0.97 <0.0001		0.98 <0.0001		0.99 <0.0001		0.97 <0.0001	
Climate indices	0.71 0.0001	0.65 0.0018	0.78 <0.0001	0.73 0.0002	0.73 0.0002	0.67 0.0009	0.53 0.0130	0.43 0.0542

particularly weak upwelling in 1992, 1995, 1998, 2005, and 2010. Between years, there appears to be more variability in upwelling. MOCI1-spring showed elevated sea level and SST in 1992, 1998, and 2005–2006, and low sea level and cold SST in 1991, 1999, 2001–2002, and 2008. The trend for MOCI1-spring was for lower sea level and SST through time. MOCI1-summer showed warming in 1997 and 2004 and cooling in 1994, 1996, 2000–2001, and 2010. The overall trend for MOCI1-summer was for ocean cooling, but this was driven largely by 2010. MOCI1-fall showed weak upwelling in 1992, 1997, and 2002, and particularly strong upwelling in 1990, 1998, 2000, and 2007. There was no overall trend in upwelling for MOCI1-fall.

The full MOCI time series is shown in Fig. 9. Years generally categorized as subtropical, warm, and rainy with weak winds and upwelling are 1992–1998 and 2003–2007. The pronounced 1997–1998 ENSO shift is clearly seen. Years generally categorized as sub-arctic and cold with strong winds and upwelling are 1990–1991, 1999–2002, and 2007–2011.

3.7. Correlations between the MOCI, large-scale climate indices, and local measurements

Seasonal sub-groups of MOCI produced from large-scale climate indices only, regional–local measurements only, and the original MOCI from all variables combined did not vary substantially from one another and were highly correlated (Table 4).

3.8. Status and trends of biological indicators

Spearman rank correlation results for trends in biological data sets are shown in Table 5. Chlorophyll increased in fall and winter between 1997 and 2011. Copepod biomass (NCI) increased in spring and summer (Fig. 10a). There was no trend in krill abundance. There was no trend in pigeon guillemot or Cassin's auklet reproductive success (Fig. 10b and c). Common murres decreased over the time series, however, while Brandt's cormorants increased (Fig. 10 d and e). All data sets with trends were detrended prior to further analysis (explained in detail in Methods). PC1$_{seabirds}$ explained 65% of the variability in the reproductive success of these four species (Fig. 10, eigenvalue = 2.61), and the loadings were highly similar between species (range = 0.45–0.53).

3.9. Correlations between environmental and biological indicators

We found strong correlations between the MOCI and copepods as well as seabirds. All seasonal copepod relationships with the seasonal MOCI1 were negative (Table 6a), with between 27% and 74% of the variance explained (Fig. 11). There were no significant correlations between seasonal NCI and MOCI2. MOCI1-spring was significantly correlated with reproductive success of all seabird species as well as PC1$_{seabirds}$ (Table 6b, Fig. 12). All relationships between the seasonal MOCI and seabird reproductive success (including PC1$_{seabirds}$) were negative indicating reduced breeding success with increasing MOCI values. MOCI1-spring explained 28%, 76%, 43%, and 37% of the variation in the breeding success

Table 5
Results of Spearman rank correlation for trends in biological time series. p-values were estimated by Monte Carlo simulation with 1000 repetitions.

Variable	Season/species	N	Spearman rho	p-value
Chlorophyll-a Concentration	Spring	14	0.41	0.14
	Summer	14	0.38	0.17
	Fall	14	0.68	0.01
	Winter	15	0.56	0.02
Northern Copepod Index (NCI)	Spring	16	0.53	0.04
	Summer	17	0.69	0.01
	Fall	17	0.29	0.22
	Winter	17	0.28	0.27
Krill Abundance		18	0.11	0.66
Seabird Reproductive Success	Common Murre	36	−0.29	0.09
	Pigeon Guillemot	37	−0.17	0.33
	Cassin's Auklet	37	−0.09	0.60
	Brandt's Cormorant	37	0.47	<0.01
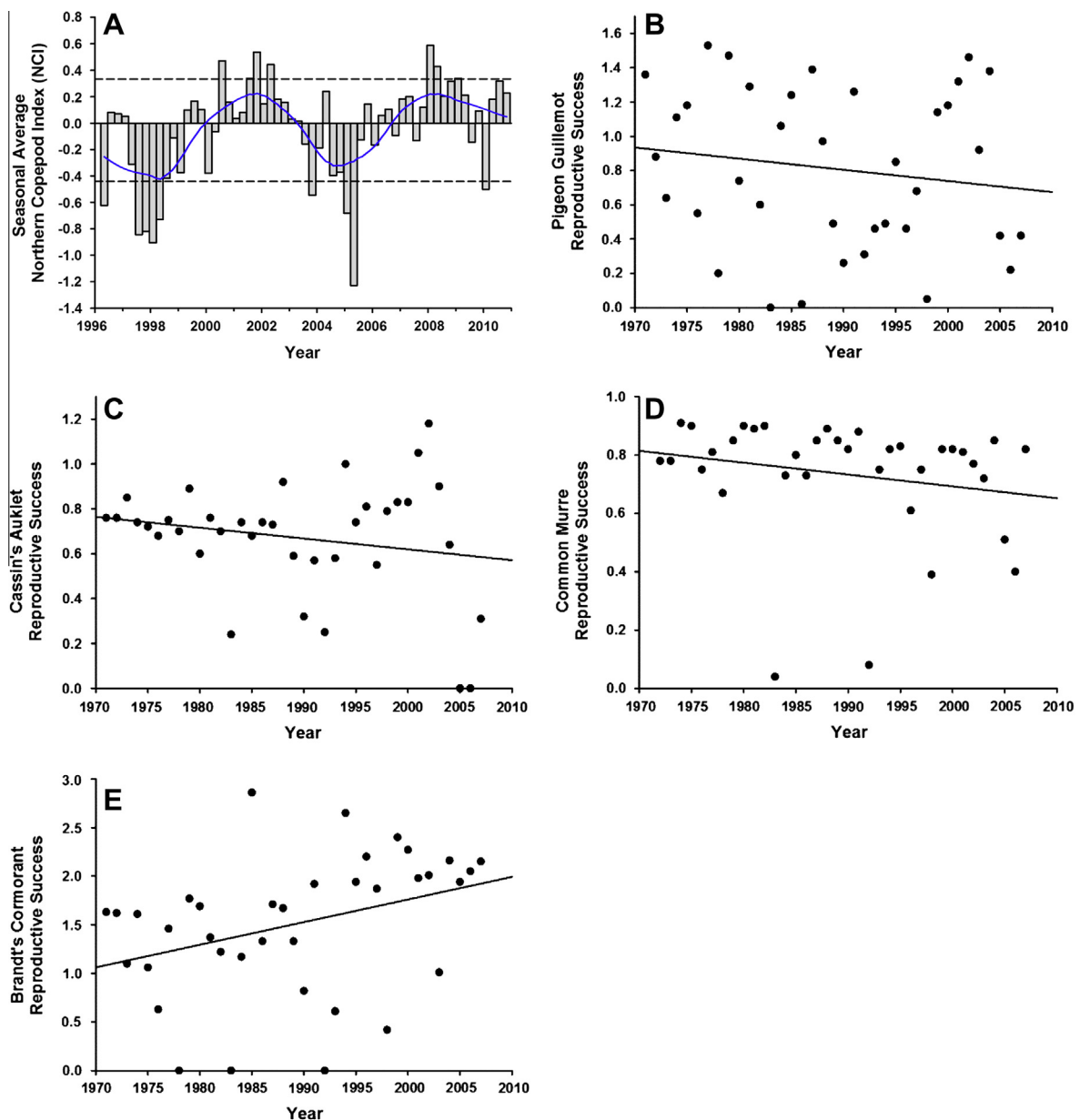
Fig. 10. (A) Seasonal average Northern Copepod Index (NCI), 1996–2010. Spring = February–April, summer = May–July, fall = August–October, and winter = November–January. The blue line indicates LOESS smoothing function with sampling proportion of 0.3. Dashed lines show ±1 standard deviation. Seabird reproductive success with linear regression for (B) pigeon guillemot (1971–2007), (C) Cassin's auklet (1971–2007), (D) common murre (1972–2007), and (E) Brandt's cormorant (1971–2007). (For interpretation of the references to color in this figure legend, the reader is referred to the web version of this article.)

Table 6
Correlations of population data and the seasonal MOCI. (A) Northern copepod index (NCI; $n = 21$). (B) Seabird reproductive success and PC1$_{seabirds}$ ($n = 40$). Biological data were detrended prior to analysis. In each cell are Spearman rho and p-value generated with Monte Carlo simulations. Shading indicates relationships where $p < 0.1$.

	MOCI1-winter	MOCI2-winter	MOCI1-spring	MOCI2-spring	MOCI1-summer	MOCI2-summer	MOCI1-fall	MOCI2-fall
(A)								
NCI spring	−0.71	0.20						
	<0.01	0.53						
NCI summer			−0.62	0.43				
			0.02	0.11				
NCI fall					−0.76	−0.19		
					<0.01	0.54		
NCI winter							−0.51	−0.41
							0.06	0.12
(B)								
Common Murre	−0.59	−0.10	−0.73	0.04	0.01	−0.57	−0.31	0.15
	0.01	0.67	<0.01	0.86	0.98	0.01	0.20	0.56
Pigeon Guillemot	−0.35	−0.03	−0.62	0.25	−0.13	−0.59	0.16	0.27
	0.13	0.92	<0.01	0.30	0.59	0.01	0.50	0.26
Cassin's Auklet	−0.19	−0.09	−0.48	−0.06	−0.50	−0.38	−0.17	0.29
	0.44	0.70	0.03	0.79	0.03	0.10	0.46	0.21
Brandt's Cormorant	−0.33	−0.13	−0.61	−0.22	−0.39	−0.66	−0.21	0.16
	0.15	0.58	<0.01	0.34	0.09	0.00	0.38	0.51
PC1$_{seabirds}$	−0.48	−0.13	−0.79	0.01	−0.44	−0.68	−0.15	0.28
	0.04	0.62	<0.01	0.97	0.07	<0.01	0.54	0.25
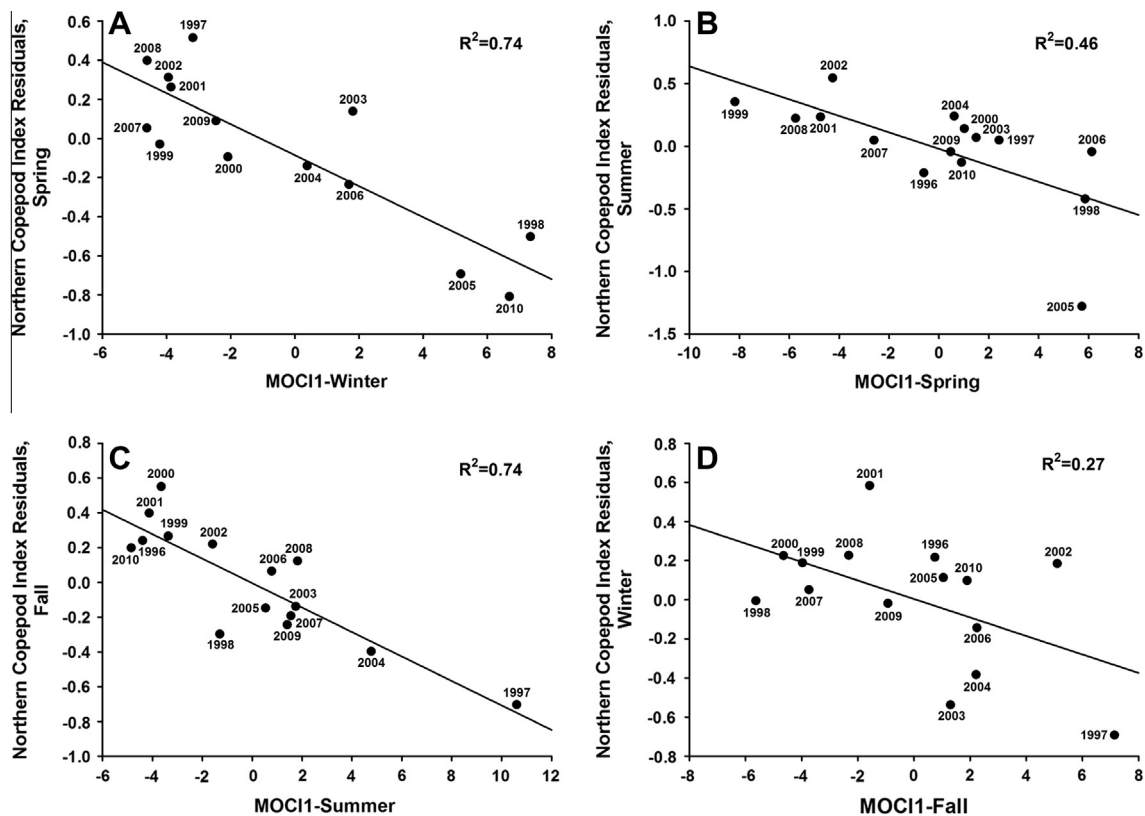
Fig. 11. Seasonal Northern Copepod Index (NCI) residuals predicted by the seasonal MOCI1, with a 1-season lag. (A) Spring copepods predicted by the winter MOCI1, (B) summer copepods predicted by the spring MOCI1, (C) fall copepods predicted by the summer MOCI1, and (D) winter copepods predicted by the fall MOCI1. Points are labeled with data year, and r^2 from linear regression is given.

of Cassin's auklet, common murre, pigeon guillemot, and Brandt's cormorant, respectively, and 59% of the variation in PC1$_{seabirds}$. There were two correlations between krill and MOCI2 (summer: $n = 18$, rho = −0.47, $p = 0.05$; fall: $n = 18$, rho = 0.52, $p = 0.03$). There were no significant relationships for krill and MOCI1, as well as no significant relationships between the seasonal MOCI and chl-a (all $p > 0.05$).

4. Discussion

Disentangling the effects of climate variability and fishing on coastal ecosystems is a challenge as both factors occur simultaneously and interact to affect food webs and biological populations (Link et al., 2002; Hsieh et al., 2008; Kenny et al., 2009; Kirby et al., 2009). As MPA designations are controversial, robust evaluations of
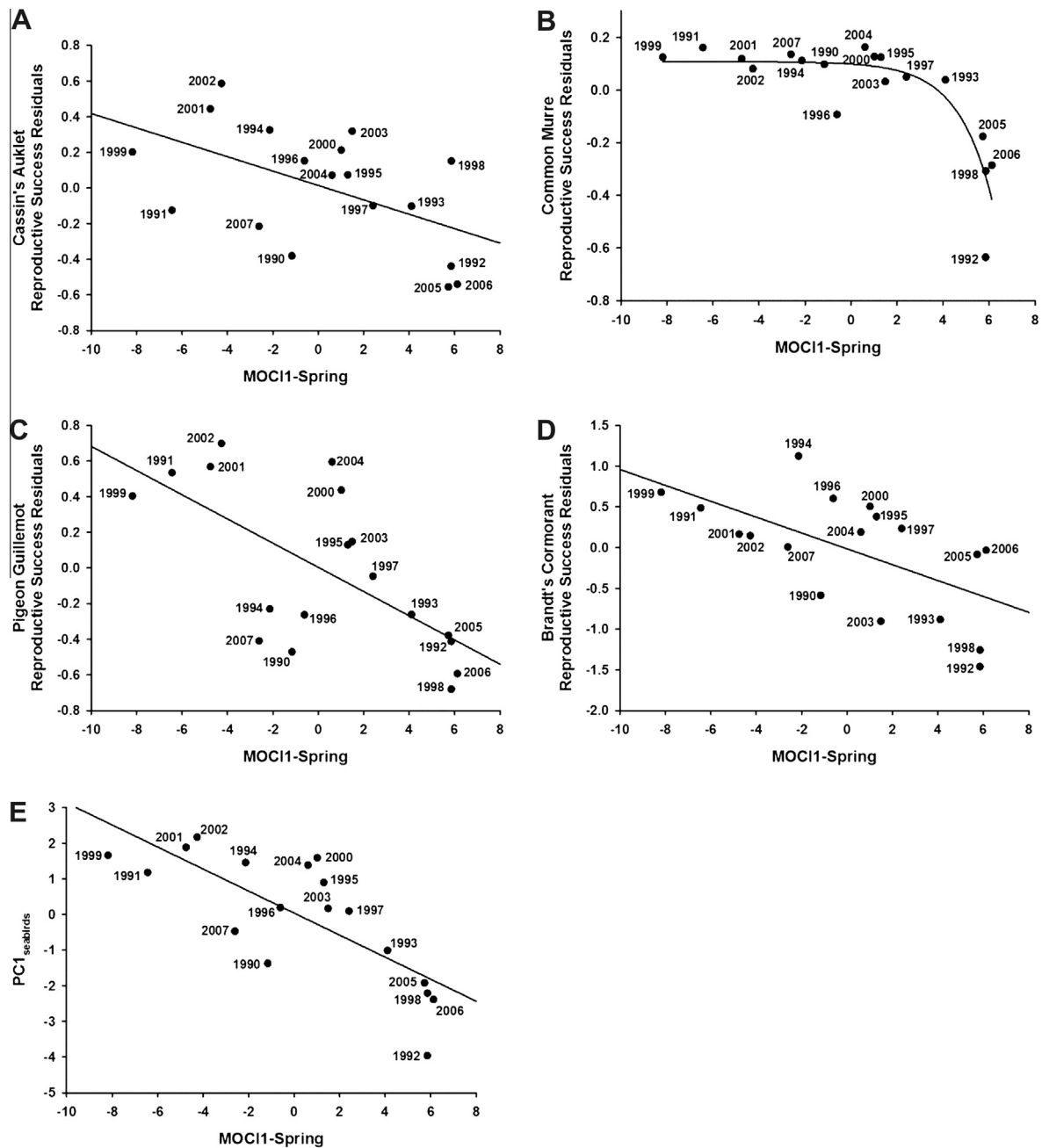
Fig. 12. Relationships for MOCI1-spring and residuals of reproductive success for (A) Cassin's auklet, (B) common murre, (C) pigeon guillemot, and (D) Brandt's cormorant. E. Relationship of the spring MOCI1 and PC1$_{seabirds}$. Regression lines are linear with the exception of common murre, which is an exponential curve.

the goals and impacts of MPAs in protecting and restoring ecosystems are needed. We implemented this study to aid in the interpretation and evaluation of ecological and biological changes within and outside newly established MPAs in the central California Current. Our primary goals were to design multivariate ecosystem indicators that capture the ocean-climate processes which affect a variety of marine life, and provide understanding of temporal environmental trends and variability in conditions during the two decades leading up to MPA designation.

4.1. Indicator design and development

To derive a description of environmental variability through time, we created seasonal multivariate indicators of environmental

conditions based on linear combinations of 14 well-known atmospheric and oceanographic indicators. In part, we modeled this work after Hemery et al. (2008) and Kenny et al. (2009), who took a similar approach to investigating coupled climate and ecosystem change in the Bay of Biscay, France, and the North Sea, respectively. Hemery et al. used 11 climate variables over four seasons (i.e., 44 variables described each year) to create their "Multivariate Ocean-Climate Index" and compared it to the major climate index of their region, the winter North Atlantic Oscillation (wNAO). Hemery et al. used SST, air temperature, precipitation, and wind variables, as we did, but we also integrated measurements of salinity, upwelling, and sea level. We used all of these variables, as well as a variety of basin-scale atmospheric and oceanographic indices (listed above), to create season-specific Multivariate Ocean

Climate Indicators ("MOCI"; winter (January–March), spring (April–June), summer (July–September), and fall (October–December)). As most biological processes and populations in the California Current are dependent on seasonal variation in environmental conditions (e.g., Abraham and Sydeman, 2004; Black et al., 2010, 2011), we surmised that deriving seasonal MOCI would be the most appropriate way to examine physical–biological interactions in this region.

By placing the seasonal values in sequence (Fig. 10), we can verify whether these indicators reflect known transitions in environmental conditions occurring during well-documented ENSO events in the eastern tropical Pacific, i.e., the strongest El Niño on record transitioning to one of the strongest La Niña events on record from 1997 to 1999 (Chavez et al., 1999). According to the MOCI, the impacts of the 1997–1998 tropical El Niño in the CCS peaked in summer 1997, then conditions transitioned to a more subarctic state in concert with the shift from tropical El Niño to La Niña in the spring of 1998. This transition is temporally matched to physical, chemical, and biological changes in the tropical Pacific and central California (Chavez et al., 2002). Similarly, a weaker, though still significant transition to an El Niño event occurred from 1991 to 1992. The seasonal MOCI indicate that this transition started in winter 1991 and peaked in winter/spring 1992. This transitional period also matched reported changes in biogeochemical attributes of the tropical Pacific (Barber et al., 1996) and central California (Chavez, 1996). A modest El Niño occurred more recently, observed in the seasonal MOCI, which peaked in winter 2010 (Bjorkstedt et al., 2012). That the MOCI match major and well-known basin-scale oceanographic transitions provides confidence that the environmental measurements selected and statistical procedures used produced indicators that accurately represent the environmental conditions in the region. The MOCI also capture the anomalous spring conditions in 2005 and 2006 that were not a result of tropical ENSO variations and therefore are not shown by the MEI, SOI, or ONI.

4.2. Relationships between indicators

A general sense of the relationships among the indicators can be interpreted from the PCA eigenvector loadings (Table 3b). First, variables with multiple sites have similar loadings. Second, SST and sea level are strongly connected. For the principal components, when sea level stands out, so does SST, and the signs are generally the same, indicating increasing temperatures with increasing sea levels, as would be expected under ENSO conditions. As previously suggested (Sydeman and Thompson, 2010), sea level is one of the best indicators available for use in environmental and ecosystem assessments as it captures variability in multiple processes including upwelling and large-scale transport (Chelton et al., 1982).

4.3. Trends in environmental conditions

The state of a marine ecosystem is a function of the forces acting upon it at various temporal and spatial scales. To assess environmental trends we selected 1990 as our cutoff due to a putative "regime shift" in environmental conditions and ecosystem status that occurred at that time (Hare and Mantua, 2000; Sydeman et al., 2001). Since 1990, the primary trend in the environment of north-central coastal California can be summarized as follows: (1) a general weakening of sub-tropical influences on the system, illustrated by declining trends in the SOI, MEI, and ONI, (2) a general strengthening of sub-arctic influences, shown by cooling of the PDO and increases in the NPGO, and (3) increasing of regional- and local-scale upwelling, the former documented by a stronger NOI and UI and the latter corresponding to changes in wind stress and SST. Interestingly, despite decreasing SST, we did not observe

trends in salinity or sea level. Some sites showed decreasing air temperature, which may be related to changes in ocean temperature. In summary, there was an increasing frequency of years of relatively strong upwelling and cold coastal SST over the 1990–2010 period. This has coincided with trends in large-scale North Pacific climate that project onto the cold phase of the PDO and an intensified gyre phase of the NPGO. Moreover, the salinity signal (see loadings on MOCI1-winter and spring in Table 3), while not reaching the criteria we considered of significance, also supports these changes. Therefore, we hypothesize that the seasonal MOCI generally track changes in sub-arctic influences on the ecosystem, and that recent large-scale changes in the North Pacific have made the central-northern California Current more temperate in nature (Sydeman et al., 2013).

4.4. Environmental transitions and sequential anomalies

The MOCI reveal rapid transitions and sequential anomalies in environmental conditions (Fig. 9). Sequential warm anomalies occurred from winter 1992 through spring 1993 (four of six seasons beyond 1 s.d. of the mean), summer 1997 through spring 1998 (all four seasons), and summer 2004 through spring 2005 (three of four seasons). A remarkably long sequence of cold anomalies occurred from fall 1998 through spring 2002, with nine of 15 seasons below 1 s.d. of the mean. Moreover, rapid transitions from cold to warm conditions were revealed from spring 1991 to winter 1992, winter to spring 1995, winter to summer 1997, and spring 2002 to winter 2003. Rapid transitions from warm to cold conditions were revealed from spring to fall 1998 and winter to summer 2010. Such long sequences of similar environmental conditions as well as periods of rapid environmental change should have important effects on populations, a point we return to below. Smoothing the seasonal MOCI reveals a generally warm period throughout most of the 1990s, a cold period in the early 2000s, a warm period in the mid 2000s, and a relatively neutral period in the late 2000s. Others have described relatively similar patterns of temporal environmental variability in the system (Bjorkstedt et al., 2012), but based only on single variables. The transitions we found, especially the rapid transition from El Niño to La Niña conditions in 1997–1999, have also been described elsewhere (Bograd and Lynn, 2001; Lavaniegos et al., 2002). Following this abrupt transition, the relatively cold period that followed led some authors to speculate that a long-term shift in environmental conditions and ecosystem state was initiated in 1999 (Peterson and Schwing, 2003; Cloern et al., 2010). The MOCI support this hypothesis in that cold conditions were apparent from 1999 to 2002 and again from 2007 through early 2011, but it is still too early to conclude that we entered a new environmental regime following the 1997–1998 ENSO. As the MOCI reflect well-documented abrupt and longer-term environmental transitions and variability, this provides confidence that our variable selection and multivariate analysis procedures were valid, and that the index produced is valuable. Abrupt transitions and sequential anomalies are undoubtedly important to populations, but it is beyond the scope of this paper to examine this idea in detail.

4.5. Linking environmental and biological indicators

While the MOCI match previously described environmental fluctuations, their linkage to populations was not as clear. Some populations related extremely well to the seasonal MOCI, while correlations with others were weak or non-existent. The MOCI had no skill in predicting variability of bulk phytoplankton biomass derived from satellite measurements. Similarly, Kim et al. (2009) found that physical variables, including upwelling winds, did not explain phytoplankton blooms off southern California. We found an increasing trend in chl-a which may be related to positive

trends in increasing wind stress (and decreasing SST; Table 2; Wilkerson et al., 2006), however, the positive relationship between chl-a and wind stress that is prevalent in nutrient-limited domains turns into a negative relationship in deeply mixed and therefore light-limited domains (Kahru et al., 2010). Importantly, on the interannual time scale (after detrending) we found no correlations between the seasonal MOCI and chl-a. Moreover, a peak in chl-a was observed during the 2004–2006 period when the MOCI generally indicated warm, weak upwelling conditions. The lack of skill of the MOCI relating to phytoplankton is most likely because of the nonlinear effect of upwelling strength on local phytoplankton biomass and spatial aliasing, i.e., more positive effects downstream of the upwelling areas. Also, the bulk chl-a does not provide information on phytoplankton community composition. It is well-known that phytoplankton species respond differently to transport, upwelling, and variation in local hydrographic conditions (Chavez et al., 2011). Furthermore, there is a spatial–temporal scaling problem in that regionally averaged indices (both physical and of chl-a) do not resolve the temporal relationship of phytoplankton blooms with wind events and stratification conditions (García-Reyes et al., in press) or with the spatial distribution of upwelling centers and retention zones (Vander Woude et al., 2006).

Seasonal variability in copepod biomass was well-explained by seasonal MOCI. The NCI represents biomass of lipid-rich cold-water copepod species that support upper trophic level predators such as salmon (Peterson and Schwing, 2003). The NCI has been previously shown to relate well to the PDO as well as alongshore transport (Hooff and Peterson, 2006) and basin-scale forcing (Bi et al., 2011), variables integrated by the MOCI. We demonstrate that these sub-arctic copepod species correlate as well or better with this complex representation of environmental variability than single physical parameters on semi-annual scales. It is worth nothing that these relationships are significantly stronger with a temporal lag of one season, suggesting that the copepod community takes time to respond to environmental variability; this is expected given their 30–45 day life cycle. As a key part of the coastal food web, predicting variability in copepods has important implications for higher trophic levels. MOCI show great skill in representing them which suggests potential for MOCI in relation to the trophic level species of management and conservation concern.

Seasonal MOCI, however, did not capture variability in krill populations very well. Despite finding relationships with MOCI2 (summer and fall), these correlations had opposing signs. We also interpret MOCI2 as an index of atmospheric conditions (temperature and precipitation), so we are unsure of the possible connection, if any, to krill populations. Moreover, the krill data in this study were produced from sampling conducted in May–June, and these annual values were compared to the seasonal MOCI. Therefore, these relationships are probably spurious. García-Reyes et al. (in press) have shown that krill populations in this area relate best with upwelling indices that consider the alternation of upwelling and relaxation events and incorporate local winds and water temperature at the time scale of days to weeks. Thus, by integrating indicators across seasons, skill in predicting krill may be lost. The life cycle of an individual krill is on the order of 4–6 months. This is strongly cohort-driven in that reproduction is strongly linked to the upwelling season, with egg production occurring mostly during large blooms associated with relaxation of upwelling in spring and summer. Thus, biomass observed in a May–June survey would not include the cohort produced at that time because juveniles and adults resulting from eggs produced in May and June, for example, would not become significant contributors to krill biomass until autumn.

Last, the seabird productivity indicators were strongly associated with seasonal MOCI, with spring explaining a significant portion of the variability in species-specific and combined seabird breeding success. Seabird breeding success in itself is an integration of a several parameters including the number of eggs produced per nest (clutch size), the proportion of eggs hatched, and the proportion of hatched chicks raised to independence (Sydeman et al., 2001). Seabird breeding success has been presented previously as an indicator of prey abundance (Cairns, 1987; Piatt et al., 2007), specifically mesozooplankton (e.g., krill) and small forage fish used for offspring production (Sydeman et al., 2013). Therefore, the strong connection between seabird breeding success and spring MOCI, coupled with the tight connections between MOCI NCI, suggests that MOCI indicate structure of coastal food webs. Importantly, this provides support for our approach in both designing and implementing the MOCI. The seabird correlations also support our contention that the lack of correlation with bulk chl-a may be due to poor information content about which species of phytoplankton are represented in the chl-a values obtained via satellite remote-sensing. It is apparent that the copepod and seabird variables contain some integrative characteristic similar to that of MOCI, which apparently differs from the other biological indices considered (krill and chl-a).

5. Conclusion

We designed and implemented multivariate indicators of ocean climate (MOCI) for the central-northern California Current based on processes known to affect ecosystem dynamics (transport from the south and north and regional upwelling). The seasonal MOCI represent environmental variability well and show promise for understanding physical-biological interactions in the system. Therefore, the MOCI should be useful in the evaluation of management actions aimed at improving populations. Furthermore, with relative ease and minimal cost, it is possible to develop automated script to maintain and provide updated MOCI to the research and management community.

References

Abraham, C.L., Sydeman, W.J., 2004. Ocean climate, euphausiids and auklet nesting: inter-annual trends and variation in phenology, diet and growth of a planktivorous seabird, *Ptychoramphus aleuticus*. Marine Ecology Progress Series 274, 235–250.

Barber, R.T., Sanderson, M.P., Lindley, S.T., Chai, F., Newton, J., Trees, C.C., Foley, D.G., Chavez, F.P., 1996. Primary productivity and its regulation in the equatorial Pacific during and following the 1991–1992 El Niño. Deep-Sea Research Part II 43, 933–969.

Beaugrand, G., Brander, K.M., Lindley, J.A., Souissi, S., Reid, P.C., 2003. Plankton effect on cod recruitment in the North Sea. Nature 426, 661–664.

Bi, H., Peterson, W.T., Strub, P.T., 2011. Transport and coastal zooplankton communities in the northern California Current system. Geophysical Research Letters 38, L12607.

Bjorkstedt, E.P., Goericke, R., McClatchie, S., Weber, E., Watson, W., Lo, N., Peterson, B., Emmett, B., Peterson, J., Durazo, R., Gaxiola-Castro, G., Chavez, F., Pennington, J.T., Collins, C.A., Field, J., Ralston, S., Sakuma, K., Bograd, S.J., Schwing, F.B., Xue, Y., Sydeman, W.J., Thompson, S.A., Santora, J.A., Largier, J., Halle, C., Morgan, S., Kim, S.Y., Merkens, K.P.B., Hildebrand, J.A., Munger, L.M., 2010. State of the California Current 2009–2010: regional variation persists through transition from La Niña to El Niño (and back?). California Cooperative Oceanic Fisheries Investigations Report 51, 39–69.

Bjorkstedt, E.P., Goericke, R., McClatchie, S., Weber, E., Watson, W., Lo, N., Peterson, B., Brodeur, R., Bograd, S., Auth, T., Fisher, J., Morgan, C., Peterson, J., Durazo, R., Gaxiola-Castro, G., Lavaniegos, B., Chavez, F., Collins, C.A., Hannah, B., Field, J., Sakuma, K., Satterthwaite, W., O'Farrell, M., Sydeman, W.J., Thompson, S.A., Warzybok, P., Bradley, R., Jahncke, J., Golightly, R., Schneider, S., Largier, J., Kim, S.Y., Melin, S., DeLong, R., Abell, J., 2012. State of the California Current 2011–2012: ecosystems respond to local forcing as La Niña wavers and wanes. California Cooperative Oceanic Fisheries Investigations Reports 53, 41–76.

Black, B.A., Schroeder, I.D., Sydeman, W.J., Bograd, S.J., Lawson, P.W., 2010. Wintertime ocean conditions synchronize rockfish growth and seabird reproduction in the central California Current ecosystem. Canadian Journal of Fisheries and Aquatic Sciences 67, 1149–1158.

Black, B.A., Schroeder, I.D., Sydeman, W.J., Bograd, S.J., Wells, B.K., Schwing, F.B., 2011. Winter and summer upwelling modes and their relevance to climate impacts and ecological response in the California Current Ecosystem. Global Change Biology 17, 2536–2545.

Bograd, S.J., Lynn, R.J., 2001. Physical-biological coupling in the California Current during the 1997–99 El Niño–La Niña cycle. Geophysical Research Letters 28, 275–278.

Bograd, S.J., Schroeder, I., Sarkar, N., Qiu, X.M., Sydeman, W.J., Schwing, F.B., 2009. Phenology of coastal upwelling in the California Current. Geophysical Research Letters 36, L01602.

Bond, N.A., Overland, J.E., Spillane, M., Stabeno, P.J., 2003. Recent shifts in the state of the North Pacific. Geophysical Research Letters 30, 2183.

Cairns, D.K., 1987. Seabirds as indicators of marine food supplies. Biological Oceanography 5, 261–271.

Carr, M.H., Woodson, C.B., Cheriton, O.M., Malone, D., McManus, M.A., Raimondi, P.T., 2011. Knowledge through partnerships: integrating marine protected area monitoring and ocean observing systems. Frontiers in Ecology and the Environment 9, 342–350.

Chavez, F.P., 1996. Forcing and biological impact of onset of the 1992 El Niño in central California. Geophysical Research Letters 23, 265–268.

Chavez, F.P., Strutton, P.G., Friederich, G.E., Feely, R.A., Feldman, G.C., Foley, D.G., McPhaden, M.J., 1999. Biological and chemical response of the Equatorial Pacific Ocean to the 1997–98 El Niño. Science 286, 2126–2131.

Chavez, F.P., Pennington, J.T., Castro, C.G., Ryan, J.P., Michisaki, R.P., Schlining, B., Walz, P., Buck, K.R., McFadyen, A., Collins, C.A., 2002. Biological and chemical consequences of the 1997–1998 El Niño in central California waters. Progress in Oceanography 54, 205–232.

Chavez, F.P., Messie, M., Pennington, J.T., 2011. Marine primary production in relation to climate variability and change. Annual Review of Marine Science 3, 227–260.

Checkley, D.M., Barth, J.A., 2009. Patterns and processes in the California Current System. Progress in Oceanography 83, 49–64.

Chelton, D.B., Bernal, P.A., McGowan, J.A., 1982. Large-scale interannual physical and biological interactions in the California Current. Journal of Marine Research 40, 1095–1125.

Cloern, J.E., Hieb, K.A., Jacobson, T., Sanso, B., Di Lorenzo, E., Stacey, M.T., Largier, J.L., Meiring, W., Peterson, W.T., Powell, T.M., Winder, M., Jassby, A.D., 2010. Biological communities in San Francisco Bay track large-scale climate forcing over the North Pacific. Geophysical Research Letters 37, L21602.

Cury, P.M., Shin, Y.J., Planque, B., Durant, J.M., Fromentin, J.M., Kramer-Schadt, S., Stenseth, N.C., Travers, M., Grimm, V., 2008. Ecosystem oceanography for global change in fisheries. Trends in Ecology & Evolution 23, 338–346.

Di Lorenzo, E., Schneider, N., Cobb, K.M., Franks, P.J.S., Chhak, K., Miller, A.J., McWilliams, J.C., Bograd, S.J., Arango, H., Curchitser, E., Powell, T.M., Riviere, P., 2008. North Pacific Gyre Oscillation links ocean climate and ecosystem change. Geophysical Research Letters 35, L08607.

Field, J.C., MacCall, A.D., Bradley, R.W., Sydeman, W.J., 2010. Estimating the impacts of fishing on dependent predators: a case study in the California Current. Ecological Applications 20, 2223–2236.

García-Reyes, M., Largier, J., 2010. Observations of increased wind-driven coastal upwelling off central California. Journal of Geophysical Research 115, C04011.

García-Reyes, M., Largier, J.L., 2012. Seasonality of coastal upwelling off central and northern California: new insights, including temporal and spatial variability. Journal of Geophysical Research 117, C03028.

García-Reyes, M., Largier, J.L., Sydeman, W.J., 2013. High-frequency upwelling indices predict lower trophic level productivity. Progress in Oceanography (in press), http://dx.doi.org/10.1016/j.pocean.2013.08.004.

GRL Special Section, 2006. Warm ocean conditions in the California Current in spring/summer 2005: causes and consequences. Geophysical Research Letters 33(22).

Hare, S.R., Mantua, N.J., 2000. Empirical evidence for North Pacific regime shifts in 1977 and 1989. Progress in Oceanography 47, 103–145.

Hemery, G., D'Amico, F.D., Castege, I., Dupont, B., D'Elbee, J., Lalanne, Y., Mouches, C., 2008. Detecting the impact of oceano-climatic changes on marine ecosystems using a multivariate index: the case of the Bay of Biscay (North Atlantic-European Ocean). Global Change Biology 14, 27–38.

Hjort, J., 1914. Fluctuations in the great fisheries of northern Europe viewed in the light of biological research. Rapport et Proces-verbaux des Reunions, Conseil International pour l'Exploration de la Mer 20, 1–228.

Hooff, R.C., Peterson, W.T., 2006. Copepod biodiversity as an indicator of changes in ocean and climate conditions of the northern California current ecosystem. Limnology and Oceanography 51, 2607–2620.

Hsieh, C.H., Reiss, C.S., Hewitt, R.P., Sugihara, G., 2008. Spatial analysis shows that fishing enhances the climatic sensitivity of marine fishes. Canadian Journal of Fisheries and Aquatic Sciences 65, 947–961.

Huyer, A., 1983. Coastal upwelling in the California Current System. Progress in Oceanography 12, 259–284.

Kahru, M., Gille, S.T., Murtugudde, R., Strutton, P., Manzano-Sarabia, M., Wang, H., Mitchell, B.G., 2010. Global correlations between winds and ocean chlorophyll. Journal of Geophysical Research 115, C12040.

Kahru, M., Kudela, R.M., Manzano-Sarabia, M., Mitchell, B.G., 2012. Trends in the surface chlorophyll of the California Current: merging data from multiple ocean color satellites. Deep-Sea Research Part II 77–80, 89–98.

Keister, J.E., Di Lorenzo, E., Morgan, C.A., Combes, V., Peterson, W.T., 2011. Zooplankton species composition is linked to ocean transport in the Northern California Current. Global Change Biology 17, 2498–2511.

Kenny, A.J., Skjoldal, H.R., Engelhard, G.H., Kershaw, P.J., Reid, J.B., 2009. An integrated approach for assessing the relative significance of human pressures and environmental forcing on the status of Large Marine Ecosystems. Progress in Oceanography 81, 132–148.

Kim, H.-J., Miller, A.J., McGowan, J., Carter, M.L., 2009. Coastal phytoplankton blooms in the Southern California Bight. Progress in Oceanography 82, 137–147.

Kirby, R.R., Beaugrand, G., Lindley, J.A., 2009. Synergistic effects of climate and fishing in a marine ecosystem. Ecosystems 12, 548–561.

Lavaniegos, B.E., Jimenez-Perez, L.C., Gaxiola-Castro, G., 2002. Plankton response to El Niño 1997–1998 and La Niña 1999 in the southern region of the California Current. Progress in Oceanography 54, 33–58.

Lenarz, W.H., Ventresca, D.A., Graham, W.M., Schwing, F.B., Chavez, F., 1995. Explorations of El Niño events and associated biological population dynamics off central California. California Cooperative Oceanic Fisheries Investigations Reports 36, 106–119.

Levin, P.S., Fogarty, M.J., Murawski, S.A., Fluharty, D., 2009. Integrated Ecosystem Assessments: developing the scientific basis for ecosystem-based management of the ocean. PLoS Biology 7, 23–28.

Link, J.S., Brodziak, J.K.T., Edwards, S.F., Overholtz, W.J., Mountain, D., Jossi, J.W., Smith, T.D., Fogarty, M.J., 2002. Marine ecosystem assessment in a fisheries management context. Canadian Journal of Fisheries and Aquatic Sciences 59, 1429–1440.

Mackas, D.L., Batten, S., Trudel, M., 2007. Effects on zooplankton of a warmer ocean: recent evidence from the Northeast Pacific. Progress in Oceanography 75, 223–252.

Manly, B.F.J., 2007. Randomization, Bootstrap and Monte Carlo Methods in Biology. Chapman & Hall/CRC, Taylor & Francis Group, L.L.C., Boca Raton, Florida.

Mantua, N.J., Hare, S.R., Zhang, Y., Wallace, J.M., Francis, R.C., 1997. A Pacific interdecadal climate oscillation with impacts on salmon production. Bulletin of the American Meteorological Society 78, 1069–1079.

McGowan, J.A., Bograd, S.J., Lynn, R.J., Miller, A.J., 2003. The biological response to the 1977 regime shift in the California Current. Deep-Sea Research Part II 50, 2567–2582.

McPhaden, M.J., Zebiak, S.E., Glantz, M.H., 2006. ENSO as an integrating concept in Earth science. Science 314, 1740–1745.

NOS, 2008. CO-OPS Specifications and Deliverables for Installation, Operation, and Removal of Water Level Stations. Requirements and Developmental Division, Center for Operational Oceanographic Products and Services, National Ocean Service, NOAA.

Peña, M.A., Bograd, S.J., 2007. Time series of the northeast Pacific. Progress in Oceanography 75, 115–119.

Peterson, W.T., Schwing, F.B., 2003. A new climate regime in Northeast Pacific ecosystems. Geophysical Research Letters 30, 1896.

Piatt, J.F., Harding, A.M.A., Shultz, M., Speckman, S.G., Van Pelt, T.I., Drew, G.S., Kettle, A.B., 2007. Seabirds as indicators of marine food supplies: Cairns revisited. Marine Ecology Progress Series 352, 221–234.

Ralston, S., Sakuma, K.M., Field, J.C., 2013. Interannual variation in pelagic juvenile rockfish (Sebastes spp.) abundance – going with the flow. Fisheries Oceanography 22, 288–308.

Rice, J.C., Rochet, M.J., 2005. A framework for selecting a suite of indicators for fisheries management. ICES Journal of Marine Science 62, 516–527.

Santora, J.A., Field, J.C., Schroeder, I.D., Sakuma, K., Wells, B.K., Sydeman, W.J., 2012. Spatial ecology of krill, micronekton and top predators in the central California Current: defining ecologically important areas. Progress in Oceanography 106, 154–174.

Sakuma, K.M., Ralston, S., Wespestad, V.G., 2006. Interannual and spatial variation in the distribution of young-of-the-year rockfish (Sebastes spp.): expanding and coordinating a survey sampling frame. California Cooperative Oceanic Fisheries Investigations Reports 47, 127–139.

Schroeder, I.D., Hazen, E.L., Black, B.A., Bograd, S.J., Sydeman, W.J., Santora, J.A., Wells, B.K., 2013. Deconstructing the North Pacific High. Geophysical Research Letters 40, 541–546.

Schwing, F.B., O'Farrell, M., Steger, J.M., Baltz, K., 1996. Coastal Upwelling Indices, West Coast of North America, 1946–1995. NOAA-TM-NMFS-SWFSC-231.

Schwing, F.B., Murphree, T., deWitt, L., Green, P.M., 2002. The evolution of oceanic and atmospheric anomalies in the northeast Pacific during the El Niño and La Niña events of 1995–2001. Progress in Oceanography 54, 459–491.

Schwing, F.B., Bond, N.A., Bograd, S.J., Mitchell, T., Alexander, M.A., Mantua, N., 2006. Delayed coastal upwelling along the US West Coast in 2005: a historical perspective. Geophysical Research Letters 33, L22S01.

Sydeman, W.J., Thompson, S.A., 2010. The California Current Integrated Ecosystem Assessment (IEA), Module II: Trends and Variability in Climate-Ecosystem State.

Report to NOAA, SWFSC, Environmental Research Division. Pacific Grove, California.

Sydeman, W.J., Hester, M., Thayer, J.A., Gress, F., Martin, P., Buffa, J., 2001. Climate change, reproductive performance and diet composition of marine birds in the southern California Current System, 1967–1997. Progress in Oceanography 49, 309–329.

Sydeman, W.J., Santora, J.A., Thompson, S.A., Marinovic, B., Di Lorenzo, E., 2013. Increasing variance in North Pacific climate explains unprecedented ecosystem variability off California. Global Change Biology 19, 1662–1675.

Thompson, S.A., Sydeman, W.J., Santora, J.A., Black, B.A., Suryan, R.M., Calambokidis, J., Peterson, W.T., Bograd, S.J., 2012. Linking predators to seasonality of upwelling: using food web indicators and path analysis to infer trophic connections. Progress in Oceanography 101, 106–120.

Vander Woude, A.J., Largier, J.L., Kudela, R.M., 2006. Nearshore retention of upwelled waters north and south of Point Reyes (northern California). Deep-Sea Research Part II 53, 2985–2998.

Wilkerson, F.P., Lassiter, A.M., Dugdale, R.C., Marchi, A., Hogue, V.E., 2006. The phytoplankton bloom response to wind events and upwelled nutrients during the CoOP WEST study. Deep-Sea Research Part II 53, 3023–3048.

Wolter, K., Timlin, M.S., 1993. Monitoring ENSO in COADS with a seasonally adjusted principal component index. In: Proceedings of the 17th Climate Diagnostics Workshop, Norman, Oklahoma, pp. 52–57.

Zhang, Y., Wallace, J.M., Battisti, D.S., 1997. ENSO-like interdecadal variability: 1900–93. Journal of Climate 10, 1004–1020.